

# H<sub>2</sub>CHXdedpa and H<sub>4</sub>CHXoctapa—Chiral Acyclic Chelating Ligands for <sup>67/68</sup>Ga and <sup>111</sup>In Radiopharmaceuticals

Caterina F. Ramogida,<sup>†,‡</sup> Jacqueline F. Cawthray,<sup>†</sup> Eszter Boros,<sup>†,‡</sup> Cara L. Ferreira,<sup>§</sup> Brian O. Patrick,<sup>†</sup> Michael J. Adam,<sup>\*,‡</sup> and Chris Orvig<sup>\*,†</sup>

<sup>†</sup>Medicinal Inorganic Chemistry Group, Department of Chemistry, University of British Columbia, 2036 Main Mall, Vancouver, British Columbia V6T 1Z1, Canada

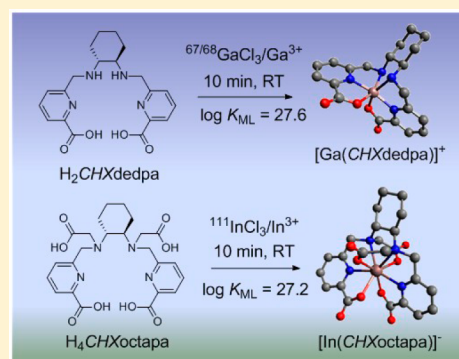
<sup>‡</sup>TRIUMF, 4004 Wesbrook Mall, Vancouver, British Columbia V6T 2A3, Canada

<sup>§</sup>Nordion, 4004 Wesbrook Mall, Vancouver, British Columbia V6T 2A3, Canada

## Supporting Information

**ABSTRACT:** The chiral acyclic ligands H<sub>2</sub>CHXdedpa (N<sub>4</sub>O<sub>2</sub>), H<sub>2</sub>CHXdedpa-bb (N<sub>4</sub>O<sub>2</sub>), and H<sub>4</sub>CHXoctapa (N<sub>4</sub>O<sub>4</sub>) (CHX = cyclohexyl/cyclohexane, H<sub>2</sub>dedpa = 1,2-[[6-carboxy-pyridin-2-yl]-methylamino]ethane, bb = *N,N'*-dibenzylated, H<sub>4</sub>octapa = *N,N'*-bis(6-carboxy-2-pyridylmethyl)-ethylenediamine-*N,N'*-diacetic acid) were synthesized, complexed with Ga(III) and/or In(III), and evaluated for their potential as chelating agents in radiopharmaceutical applications. The ligands were compared to the previously studied hexadentate H<sub>2</sub>dedpa and octadentate H<sub>4</sub>octapa ligands to determine the effect adding a chiral 1*R*,2*R*-*trans*-cyclohexane to replace the ethylenediamine backbone would have on metal complex stability and radiolabeling kinetics. It was found that [Ga(CHXdedpa)]<sup>+</sup> showed very similar properties to those of [Ga(dedpa)]<sup>+</sup>, with only one isomer in solution observed by NMR spectroscopy, and minimal structural changes in the solid-state X-ray structure.

Like [Ga(dedpa)]<sup>+</sup>, [Ga(CHXdedpa)]<sup>+</sup> exhibited exceptionally high thermodynamic stability constants (log *K*<sub>ML</sub> = 28.11(8)), and the chelate retained the ability to label <sup>67</sup>Ga quantitatively in 10 min at room temperature at ligand concentrations of 1 × 10<sup>-5</sup> M. In vitro kinetic inertness assays demonstrated the [<sup>67</sup>Ga(CHXdedpa)]<sup>+</sup> complex to be more stable than [<sup>67</sup>Ga(dedpa)]<sup>+</sup> in a human serum competition, with 90.5% and 77.8% of <sup>67</sup>Ga remaining chelate-bound after 2 h, respectively. Preliminary coordination studies of H<sub>4</sub>CHXoctapa with In(III) demonstrated [In(CHXoctapa)]<sup>-</sup> to have an equivalently high thermodynamically stable constant as [In(octapa)]<sup>-</sup>, with log *K*<sub>ML</sub> values of 27.16(9) and 26.76(14), respectively. The [<sup>111</sup>In(CHXoctapa)]<sup>-</sup> complex showed exceptionally high in vitro kinetic inertness over 120 h in human serum, comparing well with previously reported [<sup>111</sup>In(octapa)]<sup>-</sup> values, and an improved stability compared to the current industry “gold standards” 1,4,7,10-tetraazacyclododecane-1,4,7,10-tetraacetic acid (DOTA) and diethylenetriaminepentaacetic acid (DTPA). Initial investigations reveal that the chiral acyclic hexadentate H<sub>2</sub>CHXdedpa and octadentate H<sub>4</sub>CHXoctapa ligands are ideal candidates for radiopharmaceutical elaboration of gallium or indium isotopes, respectively.



## INTRODUCTION

The use of “non-traditional” radiometals in nuclear medicine has blossomed over the past decade into a well-established field that shows great utility for the diagnosis and targeted therapy of a variety of diseases, especially in the field of oncology.<sup>1–11</sup> Radioisotopes of Ga(III), In(III), Cu(II), Y(III), and Zr(IV) give a flavor of the myriad of radiometal ions that have been exploited in radiopharmaceutical design; their inherent array of nuclear decay properties and half-lives lends them well to target a variety of molecular processes.<sup>1–11</sup> Two clinically important isotopes are the positron emitter <sup>68</sup>Ga for positron-emission tomography (PET) imaging, and <sup>111</sup>In, a gamma-emitter for single-photon emitted computed tomography (SPECT) imaging and Auger electron therapy.

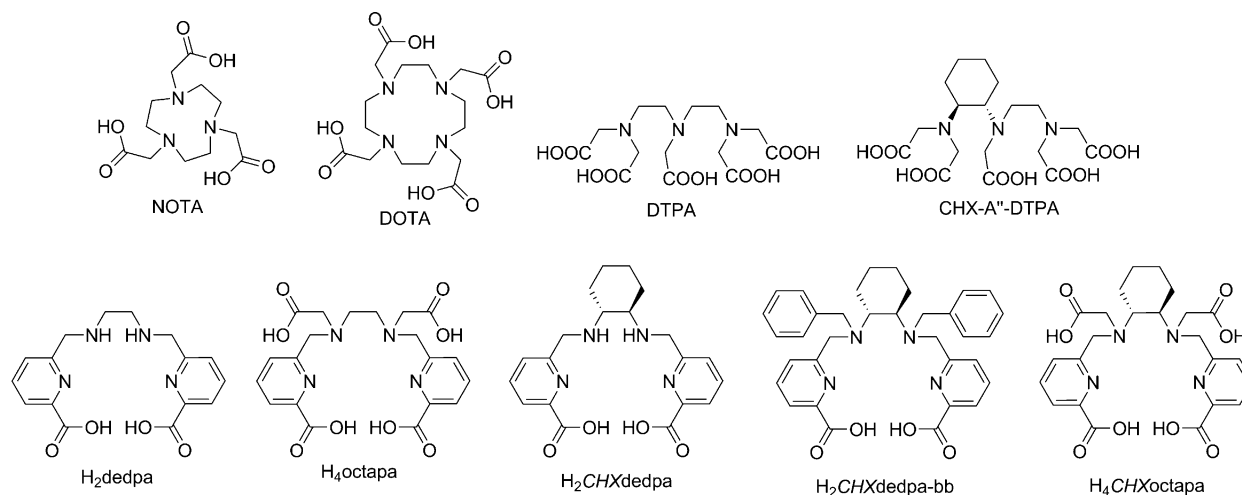
<sup>68</sup>Ga, with a short half-life suitable for imaging agents that localize quickly, such as small molecules and peptides (*t*<sub>1/2</sub> = 67.7

min), and its predominant β<sup>+</sup> emission (89%, 1.9 MeV maximum energy), has become an attractive isotope for incorporation into positron-emission tomography (PET) imaging agents.<sup>1,2,5,6,12</sup> Moreover, the nuclide <sup>68</sup>Ge/<sup>68</sup>Ga can be commercially produced and distributed via a <sup>68</sup>Ge/<sup>68</sup>Ga generator system; the half-life of the generator-parent <sup>68</sup>Ge (*t*<sub>1/2</sub> = 270 d) is sufficiently long such that the generator can be used for six months to one year before replacement,<sup>13,14</sup> obviating the need for an on-site cyclotron. Therefore, the <sup>68</sup>Ge/<sup>68</sup>Ga generator has the potential to become as ubiquitous as the clinically important <sup>99</sup>Mo/<sup>99m</sup>Tc generator, and the <sup>68</sup>Ga from these generators is already being used in patients throughout Europe. The lack of an FDA-approved

**Received:** December 9, 2014



Chart 1. Structures of Ligands Discussed in This Work



$^{68}\text{Ge}/^{68}\text{Ga}$  generator is hindering the advancement of many  $^{68}\text{Ga}$  agents toward the clinic in North America, but progress is steady.

$^{111}\text{In}$  has a half-life of  $\sim 2.8$  d, is produced by cyclotron ( $^{111}\text{Cd}(p,n)^{111}\text{In}$ ), and decays via electron capture (EC, 100%) emitting  $\gamma$ -rays with energies of 171 and 245 keV, which are sufficient for SPECT imaging, as well as Auger electrons that can be used for therapy.<sup>1,6</sup> The radiometal  $^{111}\text{In}$  is commercially available and has been incorporated into the clinically relevant agents Octreoscan and ProstaScint, with many more  $^{111}\text{In}$ -based radiopharmaceuticals in clinical trials.<sup>15</sup> It is the second most popular SPECT radiometal next to  $^{99\text{m}}\text{Tc}$ .

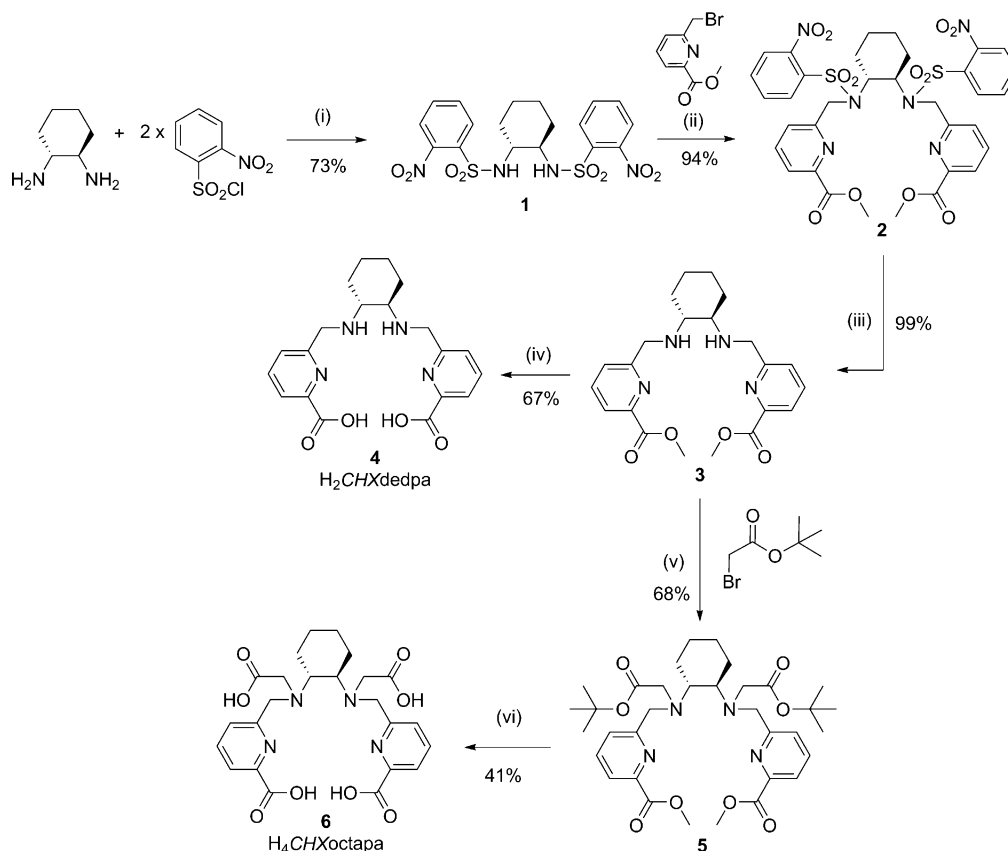
The utility of radiometals such as  $^{111}\text{In}$  and  $^{68}\text{Ga}$  in nuclear medicine is strongly dependent on a chelating ligand that exhibits rapid radiometal incorporation and strong kinetic inertness to prevent unintentional transchelation and/or demetalation of the coordination complex in vivo.<sup>5,7</sup> The tri- and tetra-aza-based aminocarboxylate macrocyclic chelators 1,4,7-triazacyclononane-1,4,7-triacetic acid (NOTA ( $\text{N}_3\text{O}_3$ )) and 1,4,7,10-tetraazacyclododecane-1,4,7,10-tetraacetic acid (DOTA ( $\text{N}_4\text{O}_4$ )), developed by Maecke and co-workers,<sup>16–18</sup> persist as the “gold-standards” in the field of radiometal chelation. NOTA and DOTA are used in many applications with their radiochemical properties ranging from sufficient to superb for many radiometals, including but not limited to  $^{64}\text{Cu}$ ,  $^{68}\text{Ga}$ ,  $^{111}\text{In}$ ,  $^{86/90}\text{Y}$ , and  $^{177}\text{Lu}$ .<sup>7</sup> The preorganized donor atoms of these macrocyclic (closed-chain) systems result in metal complexes of often very high stability; however, elevated temperatures and extended reaction times are often required to quantitatively label radiometals—a major downfall of these ligands, especially when denaturing of sensitive biomolecules and many half-lives of activity are at stake.

Many acyclic (open-chain) ligands such as diethylenetriaminepentaacetic acid (DTPA) and ethylenediaminetetraacetic acid (EDTA) have been extensively evaluated for use with a variety of radiometals,<sup>19,20</sup> and despite their rapid and quantitative radiometal incorporation, they suffer from poor kinetic inertness in vitro, a common characteristic of acyclic ligands. A structural modification of DTPA to give CHX-A''-DTPA (Chart 1) through incorporation of a 1,2-*trans*-cyclohexanediamine backbone to preorganize the donor atoms has proven to increase the kinetic inertness of its resulting metal complexes.<sup>21,22</sup> CHX-A''-DTPA has been used extensively with many radiometals including  $^{86/90}\text{Y}$ ,<sup>22,23</sup>  $^{177}\text{Lu}$ ,<sup>24,25</sup> and  $^{212/213}\text{Bi}$ ,<sup>26</sup> and some with

$^{111}\text{In}$ ,<sup>23</sup> and in most cases showed increased stability (kinetic inertness) in vivo compared to the analogous DTPA complexes.

Chelating ligand design is a key factor in radiopharmaceutical construction, and the appropriate chelate must be chosen to match the unique coordination chemistries of each metal; as such there is increasing interest in the development of new ligands that stably bind the variety of radiometal isotopes that have potential use in diagnostic imaging and targeted radiotherapy.<sup>7,27,28</sup> Many groups,<sup>29–37</sup> including ours, have sought to find new ligands with improved properties for radiometal chelation—such as fast and mild radiolabeling conditions, high thermodynamic stability, and exceptional kinetic inertness in vivo. To this end, our group has extensively studied a variety of acyclic (linear) chelators based on the pyridine carboxylate scaffold (Chart 1), which we have termed the “pa” family of chelators<sup>38–45</sup>—with the most promising entries of the family being the acyclic chelator H<sub>2</sub>dedpa and octadentate version H<sub>4</sub>octapa. We first reported the acyclic chelating ligand H<sub>2</sub>dedpa ( $\text{N}_4\text{O}_2$ ) that binds gallium isotopes quantitatively and under mild conditions with high specific activities (10 min, RT, 9.8 mCi/nmol).<sup>38</sup> Bifunctional H<sub>2</sub>dedpa derivatives were conjugated to the cyclic peptide RGD<sup>42,46</sup> and evaluated with both  $^{68}\text{Ga}$  and  $^{64}\text{Cu}$ . Moreover, monocationic Ga-dedpa derivatives with lipophilic appendages were evaluated as myocardial perfusion agents.<sup>47</sup> The octadentate version, H<sub>4</sub>octapa ( $\text{N}_4\text{O}_4$ ), was investigated for use with indium isotopes<sup>39,41</sup> and exhibited properties that rivaled those of DOTA, the current industry gold standard for indium chelation. The main advantage of the pa ligands lies in their ability to quantitatively label radiometals quickly and under mild conditions (a trait often lacking in the macrocyclic gold standards NOTA and DOTA); yet despite both being acyclic (open chain) ligands, H<sub>2</sub>dedpa and H<sub>4</sub>octapa exhibit surprisingly high kinetic inertness in vitro and in vivo.

The work presented herein is a study to investigate the effect of an added structural modification onto the backbone of these linear chelating agents. By substitution of a chiral 1*R*,2*R*-*trans*-cyclohexanediamine in place of the ethylenediamine backbone in the native scaffolds of H<sub>2</sub>dedpa and H<sub>4</sub>octapa, an augmented preorganization of the donor atoms has been enforced, which may positively affect the in vitro/in vivo kinetic inertness of the resulting metal complexes. Moreover, the replacement of ethylenediamine with a slightly more lipophilic cyclohexanediamine backbone may alter the pharmacokinetics and biodis-

Scheme 1. Synthesis of 1, 2, 3, H<sub>2</sub>CHXdedpa, 5, and H<sub>4</sub>CHXoctapa<sup>a</sup>

<sup>a</sup>Reagents and conditions: (i) THF, NaHCO<sub>3</sub>, 0 °C – RT, 18 h; (ii) CH<sub>3</sub>CN, K<sub>2</sub>CO<sub>3</sub>, methyl-6-bromomethylpicolinate (2 equiv), 65 °C, 48 h; (iii) THF, K<sub>2</sub>CO<sub>3</sub>, thiophenol (2.05 equiv), 72 h; (iv) HCl (6 M), reflux, 18 h; (v) CH<sub>3</sub>CN, Na<sub>2</sub>CO<sub>3</sub>, *tert*-butylbromoacetate (2 equiv), 60 °C, 18 h; (vi) HCl (6 M), reflux, 18 h.

tribution of the resultant radiotracers in vivo. This work has drawn inspiration from the acyclic chelator CHX-A''-DTPA, which showed much better kinetic inertness with yttrium, lutetium, and bismuth isotopes compared to the native DTPA derivative.<sup>21,48</sup>

The chelating agents investigated herein include the hexadentate (N<sub>4</sub>O<sub>2</sub>) derivatives H<sub>2</sub>CHXdedpa and H<sub>2</sub>CHXdedpa-bb, which is a model compound where benzyl groups were added to the secondary nitrogen atoms as placeholders for targeting vectors, and octadentate (N<sub>4</sub>O<sub>4</sub>) derivative H<sub>4</sub>CHXoctapa (CHX = cyclohexyl/cyclohexane, H<sub>2</sub>dedpa = 1,2-[[6-carboxy-pyridin-2-yl]-methylamino]ethane, bb = *N,N'*-dibenzylated, H<sub>4</sub>octapa = *N,N'*-bis(6-carboxy-2-pyridylmethyl)-ethylenediamine-*N,N'*-diacetic acid) (Chart 1). Much like H<sub>2</sub>dedpa and H<sub>4</sub>octapa, H<sub>2</sub>CHXdedpa has been previously investigated by other groups for coordination to divalent transition metals,<sup>49,50</sup> but to our knowledge, its coordination properties with Ga(III) have never been investigated. In addition, H<sub>4</sub>CHXoctapa is a novel ligand that has not been previously reported.

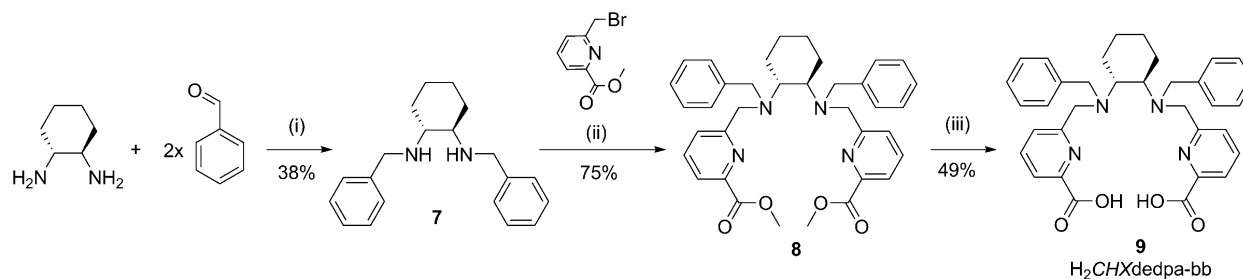
Presented herein are the synthesis, characterization, coordination chemistry, thermodynamic stability, radiolabeling, and in vitro human serum stability of the three cyclohexyl-pa ligands. These studies are used collaboratively to evaluate the potential of the CHX-pa chelates as bifunctional chelating agents in radiopharmaceutical design.

## RESULTS AND DISCUSSION

As seen in the example of the ligand CHX-DTPA and the differential stability of its four isomers,<sup>22</sup> stereochemistry can greatly influence metal–ligand complex stability in vivo. Herein we chose to focus the study on one isomer (1*R*,2*R*) of the CHX-pa chelates to eliminate any discrepancies in stability that different isomers may have, and directly compare their metal ion coordinating abilities to the previously reported achiral ethylenediamine versions.

**Synthesis and Characterization.** Like H<sub>2</sub>dedpa, H<sub>2</sub>CHXdedpa has been previously synthesized and evaluated for its chelation properties with divalent metals Zn(II), Cd(II), and Pb(II);<sup>49</sup> however, its chelation properties with gallium(III) have not yet been investigated.

Our group recently reported a novel synthesis of H<sub>2</sub>dedpa and H<sub>4</sub>octapa using the uncommon 2-nitrobenzenesulfonyl (nosyl) protecting group,<sup>41</sup> which allowed for facile and efficient preparation of both nonfunctionalized and functionalized ligands. The use of this protecting group resolved issues with the original synthetic route via the reductive amination step, which led to unwanted simultaneous reduction of the methoxy ester group. The synthesis of H<sub>4</sub>octapa or H<sub>2</sub>dedpa began with protection of ethylenediamine (en) using 2 equiv of 2-nitrobenzenesulfonyl chloride.<sup>41</sup> Herein, we prepared H<sub>2</sub>CHXdedpa in an analogous fashion (Scheme 1), with the enantiomerically pure diamine starting material 1*R*,2*R*-(−)-cyclohexanediamine being used in the first protection step with 2-nitrobenzenesulfonyl chloride to yield 1 in 73% yield. The

Scheme 2. Synthesis of 7, 8, and H<sub>2</sub>CHXdedpa-bb<sup>a</sup>

<sup>a</sup>Reagents and conditions: (i) a. Ethanol, 0 °C – reflux, 18 h, b. Ethanol, 0 °C, NaBH<sub>4</sub>, 2 h; (ii) CH<sub>3</sub>CN, K<sub>2</sub>CO<sub>3</sub>, methyl-6-bromomethyl picolinate (2.1 equiv), reflux, 72 h; (iii) THF/H<sub>2</sub>O (3:1), LiOH, RT, 2 h.

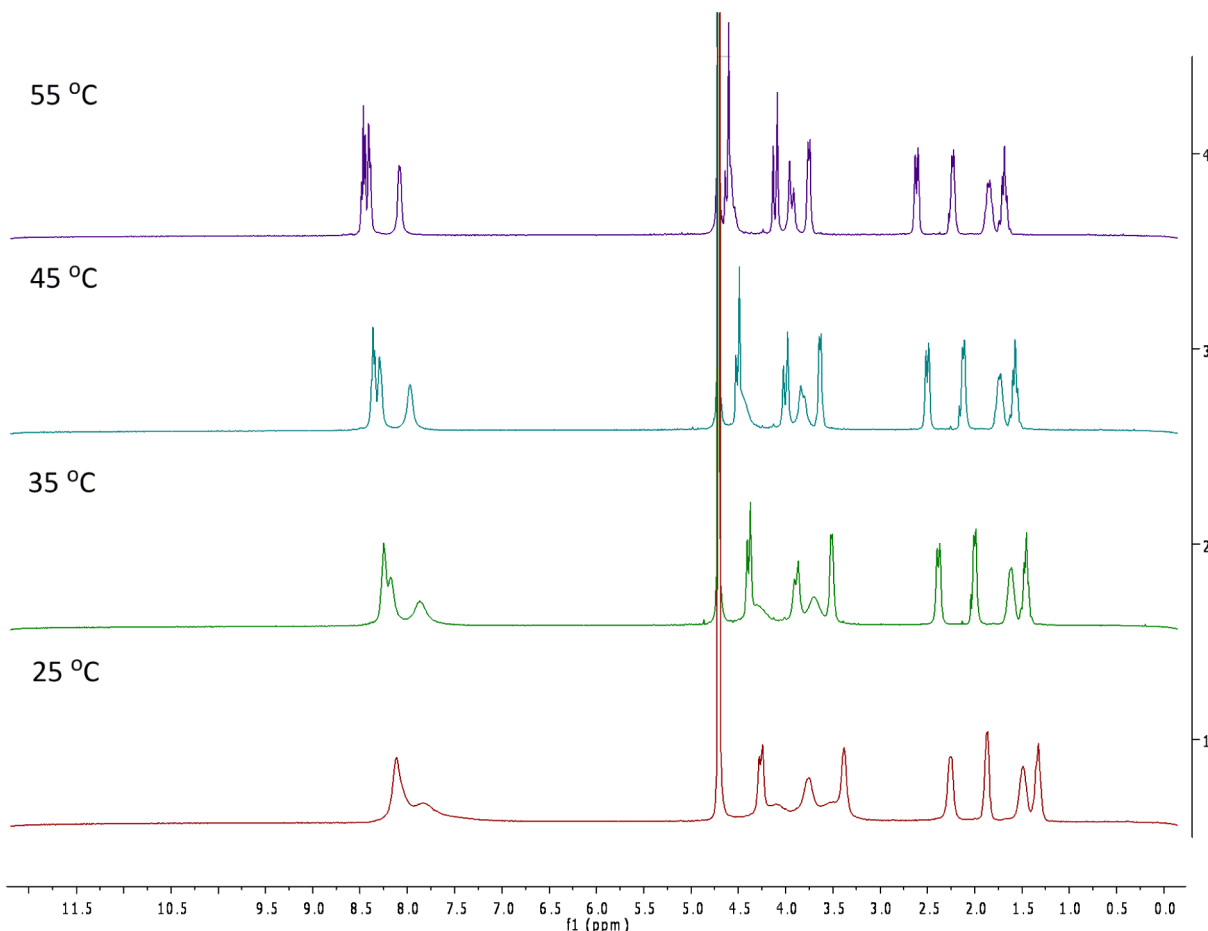
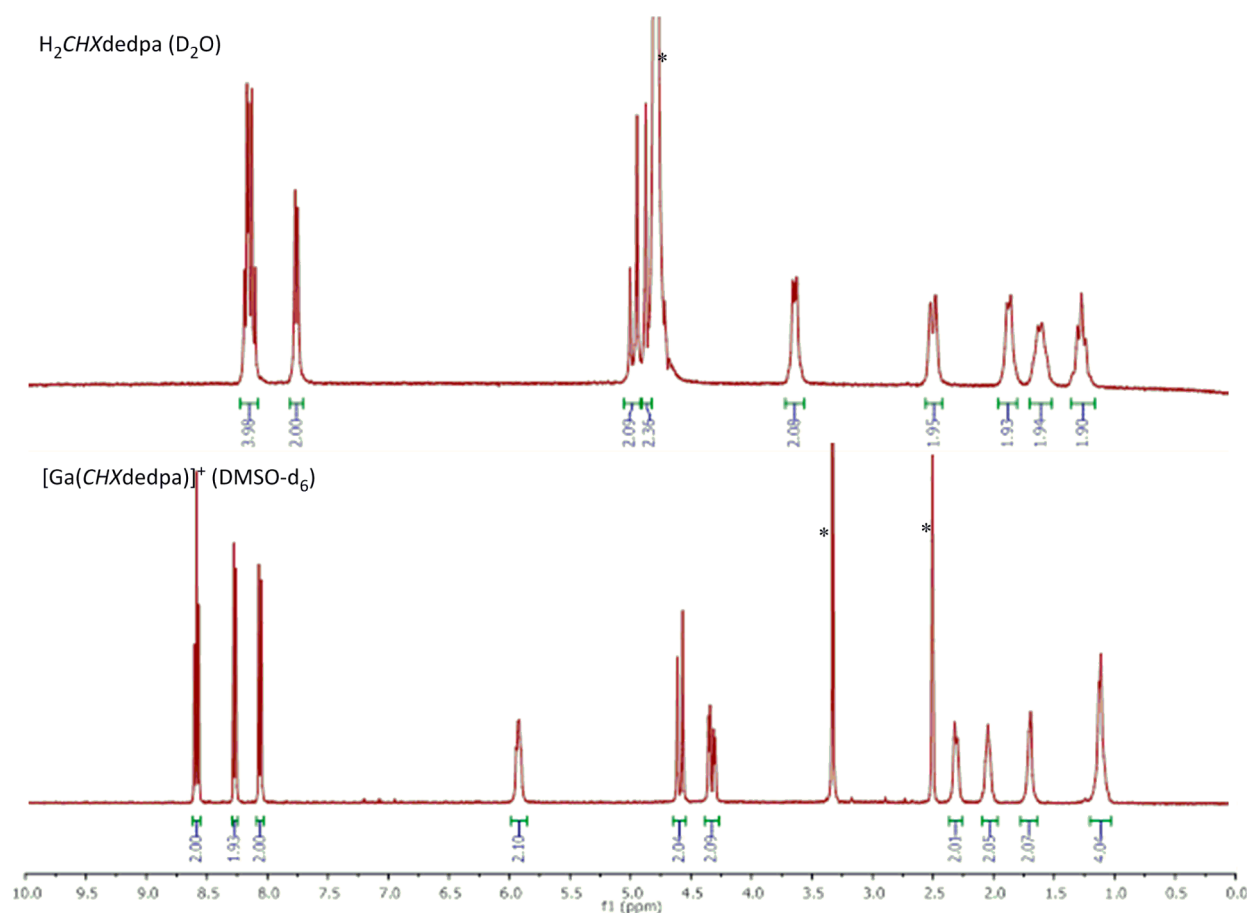


Figure 1. Variable-temperature <sup>1</sup>H NMR spectra of 6 H<sub>4</sub>CHXoctapa at 25–55 °C in D<sub>2</sub>O (400 MHz).

addition of a cyclohexyl ring on the backbone of the ethylenediamine core caused **1** to be more soluble than the ethylenediamine derivative previously reported, hence crystallization was not achieved and a column chromatography purification step was required to isolate the final protected diamine **1**. Subsequently, methyl-6-bromomethyl picolinate was used as alkylating agent, with excess base to yield **2** in high yield (94%) after column purification. The following deprotection of nosyl groups was nearly quantitative (99%) to yield Me<sub>2</sub>CHXdedpa **3**. Intermediate **3** could then be deprotected in refluxing HCl overnight to produce H<sub>2</sub>CHXdedpa as an HCl salt (46% cumulative yield in four steps), or used in a subsequent *N*-alkylation with *tert*-butyl bromoacetate (Scheme 1) to yield the protected version of

CHXoctapa<sup>4+</sup>, **5**. Finally, **5** could be deprotected in refluxing HCl to give H<sub>4</sub>CHXoctapa as an HCl salt (19% cumulative yield over five steps).

As a model for potential bifunctional derivatives of CHXdedpa<sup>2-</sup>, the dibenzylated derivative H<sub>2</sub>CHXdedpa-bb (**9**) was synthesized (Scheme 2). The benzyl groups act as placeholders for potential targeting vectors, which could be either introduced by alkylation of the 2° amines of Me<sub>2</sub>CHXdedpa (**3**) or the benzyl groups could instead be in the form of 4-nitrobenzyl groups, which would be subsequently converted to the reactive isothiocyanate for further conjugation to targeting vectors bearing reactive primary amines. A similar *N*-alkylated derivative of H<sub>2</sub>dedpa was evaluated previously, H<sub>2</sub>dedpa-bb-NO<sub>2</sub>, and found to exhibit reduced stability



**Figure 2.**  $^1\text{H}$  NMR spectra at ambient temperature of (top)  $\text{H}_2\text{CHXdedpa}$  (300 MHz) and (bottom)  $[\text{Ga}(\text{CHXdedpa})][\text{ClO}_4]$  (400 MHz) showing diastereotopic splitting present in both the free ligand and Ga complex. \*Residual solvent peak.

compared to that of  $\text{H}_2\text{dedpa}$ .<sup>38</sup> Thus,  $\text{H}_2\text{CHXdedpa-bb}$  was used to make direct comparisons to the stability trends of  $\text{H}_2\text{dedpa}$  versus  $\text{H}_2\text{dedpa-bb}$  and to determine the effect the cyclohexyl ring will have on stability of the resultant metal complex. The preparation of  $\text{H}_2\text{CHXdedpa-bb}$  (9) began with benzyl protection of  $1R,2R(-)$ -cyclohexanediamine with 2 equiv of benzaldehyde, followed by in situ reduction with sodium borohydride to produce 7. Next, methyl-6-bromomethyl picolinate was added in an alkylation step to 7 to yield the methyl-protected ligand  $\text{Me}_2\text{CHXdedpa-bb}$  (8) in 75% yield. Finally, methyl ester deprotection was accomplished in basic conditions via the addition of LiOH in water/tetrahydrofuran (THF) at room temperature. The lithium salts were removed by semipreparative RP-HPLC, and the ligand was converted to its HCl salt by redissolving in dilute HCl (aqueous). This more mild deprotection route was necessary to preserve the integrity of the ligand, since refluxing 8 in aqueous HCl resulted in debenzylation and a mixture of products.

Following synthesis, the HCl salts of all three ligands were successfully metalated with  $\text{Ga}(\text{ClO}_4)_3$  and/or  $\text{In}(\text{ClO}_4)_3$ . All proligands and their metal complexes were fully characterized using  $^1\text{H}$  NMR,  $^{13}\text{C}$  NMR,  $^1\text{H}-^1\text{H}$  COSY NMR, HSQC NMR, and high-resolution electrospray ionization mass spectrometry (HR-ESI-MS). It is interesting to note that the  $^1\text{H}$  NMR spectra of the HCl salt of  $\text{H}_4\text{CHXoctapa}$  (6) exhibited very broad and hard to resolve peaks at 25 °C, which precluded  $^{13}\text{C}$  NMR spectra collection; thus, variable-temperature (VT) NMR experiments from 25–55 °C in  $\text{D}_2\text{O}$  were performed (Figure

1). An apparent sharpening of peaks begins at 35 °C and continued as the temperature rose to 55 °C, to appear finally as sharply resolved peaks. After resolution of peaks at 55 °C was observed, a  $^{13}\text{C}$  NMR spectrum was obtained at this temperature. One explanation for this solution behavior is that there is strong intramolecular hydrogen bonding, possibly augmented by the presence of HCl, also evinced by the density functional theory (DFT) structure of  $\text{H}_4\text{CHXoctapa}$  (Supporting Information, Figure S1). This may also explain the slightly higher  $\text{pK}_a$  (vide infra) values of the ligand nitrogen atoms of  $\text{H}_4\text{CHXoctapa}$  compared to  $\text{H}_4\text{octapa}$ ; these were also corroborated by  $^1\text{H}$  NMR pH titrations at 55 °C (Supporting Information, Figure S2).

The  $^1\text{H}$  and  $^{13}\text{C}$  NMR spectra of all proligands  $\text{H}_2\text{CHXdedpa}$ ,  $\text{H}_2\text{CHXdedpa-bb}$ , and  $\text{H}_4\text{CHXoctapa}$  revealed the expected  $\text{C}_2$  symmetry with half-integrations of the resonances present and typical diastereotopic splitting of hydrogen atoms observed  $\alpha$  to the chiral center due to the inclusion of the chiral cyclohexane ring. The  $^1\text{H}$  NMR spectra at 25 °C of all Ga(chelate) complexes revealed sharp and distinct coupling patterns, and could be perceived as one electronically unique isomer in solution at ambient temperature. The  $\text{C}_2$  symmetry seen in the proligands  $\text{H}_2\text{CHXdedpa}$  and  $\text{H}_2\text{CHXdedpa-bb}$  seems to be conserved in the Ga(chelate) complexes (Figures 2 and 3, respectively). In addition, X-ray quality crystals of  $[\text{Ga}(\text{CHXdedpa})][\text{ClO}_4]$  were obtained by slow evaporation in methanol/water, the structure of which validated the solution NMR data. The solid-state structure of  $[\text{Ga}(\text{CHXdedpa})][\text{ClO}_4]$  (Figure 4) exhibited the predicted

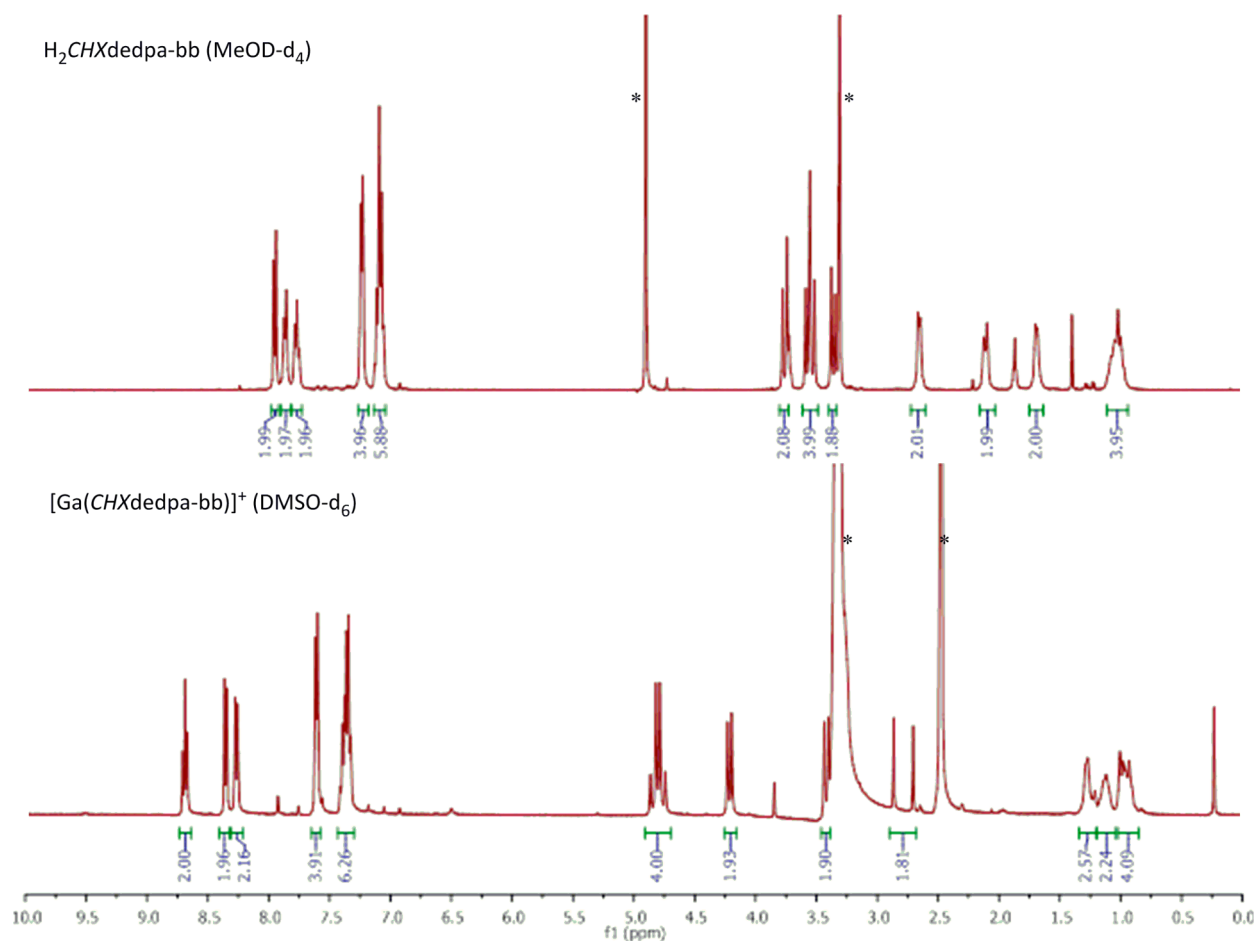


**Figure 3.** <sup>1</sup>H NMR spectra at 400 MHz of (top) H<sub>2</sub>CHXdedpa-bb and (bottom) [Ga(CHXdedpa-bb)]<sup>+</sup>[ClO<sub>4</sub>]. \*Residual solvent peak.

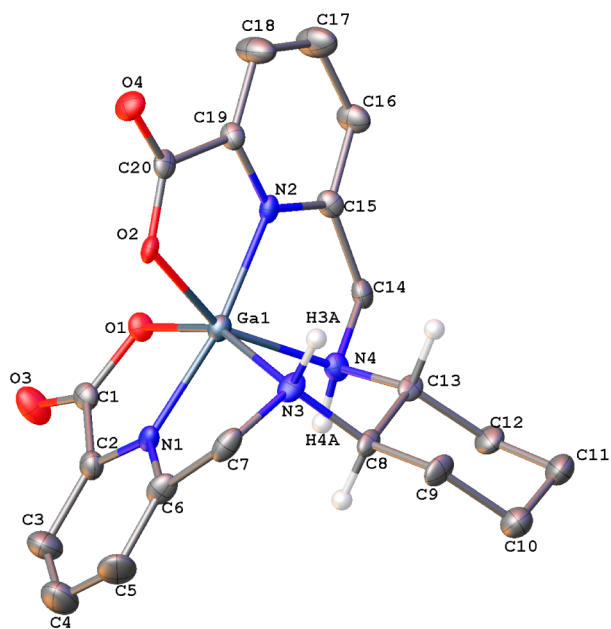


**Figure 4.** Solid-state X-ray crystal structure of the cation in [Ga(CHXdedpa)]<sup>+</sup>[ClO<sub>4</sub>]<sup>-</sup>; only one crystallographically independent unit shown; perchlorate anion omitted for clarity.

N<sub>4</sub>O<sub>2</sub> hexadentate coordination with Ga(III). There were three crystallographically independent complexes in the asymmetric unit; a comparison of relevant averaged Ga–L bond lengths and

angles of [Ga(dedpa)]<sup>+</sup> are compared with [Ga(CHXdedpa)]<sup>+</sup> in Table 1. There is very good correlation between the bond lengths and angles around the metal centers of the [Ga(CHXdedpa)]<sup>+</sup> and [Ga(dedpa)]<sup>+</sup> cations, with a maximum difference in bond length and angle of 0.032 Å and 3.3°, respectively, between all relevant Ga–L or L–Ga–L bond lengths and angles of CHXdedpa<sup>2-</sup> and dedpa<sup>2-</sup> complexes (calculated using an average of the three independent units in [Ga(CHXdedpa)]<sup>+</sup>). Because of the minor differences in bond lengths and angles, differences in dihedral angles of the two Ga complexes were also inspected; the largest difference of 9.4° is seen in the N<sub>en</sub>–C<sub>alk</sub>–C<sub>pyr</sub>–N<sub>pyr</sub> (N(3)–C(7)–C(6)–N(1)) angle between [Ga(dedpa)]<sup>+</sup> and molecule 1 of [Ga(CHXdedpa)]<sup>+</sup>, while all other relevant dihedral angles show much less variance. Though minor differences in the solid-state structures of [Ga(CHXdedpa)]<sup>+</sup> and [Ga(dedpa)]<sup>+</sup> exist, differences in stability of the metal complexes based solely on their solid-state structures cannot be discerned. Moreover, caution should always be taken when making predictions for solution-state properties based on solid-state data.

Conversely, the solution NMR spectra of [Ga(CHXoctapa)]<sup>-</sup> suggest the formation of one asymmetric isomer in solution, evinced by the apparent inequivalency of the two sets of pyridine–carboxylate hydrogens in the <sup>1</sup>H NMR spectrum (Figure 5), and 24 signals in the <sup>13</sup>C NMR spectrum, correlating to each carbon atom on the ligand backbone being electronically distinct. The splitting pattern of the pyridine–carboxylate hydrogen atoms suggests that one picolinate acid arm is

**Table 1.** Selected Bond Lengths and Angles in X-ray Structure of  $[\text{Ga}(\text{CHXdedpa})]^+$  with Comparison to  $[\text{Ga}(\text{dedpa})]^+$ 

bond	length (Å) $[\text{Ga}(\text{CHXdedpa})]^+{}^a$	length (Å) $[\text{Ga}(\text{dedpa})]^+$	bond	length (Å) $[\text{Ga}(\text{CHXdedpa})]^+{}^a$	length (Å) $[\text{Ga}(\text{dedpa})]^+$
Ga–N(1) <sub>pyr</sub>	1.968	1.9868(16)	Ga–N(4) <sub>en</sub>	2.105	2.1132(16)
Ga–N(2) <sub>pyr</sub>	1.961	1.9903(16)	Ga–O(1)	1.992	1.9708(13)
Ga–N(3) <sub>en</sub>	2.110	2.1115(16)	Ga–O(2)	1.982	1.9828(13)
angle	degree (deg) $[\text{Ga}(\text{CHXdedpa})]^+{}^a$	degree (deg) $[\text{Ga}(\text{dedpa})]^+$	angle	degree (deg) $[\text{Ga}(\text{CHXdedpa})]^+{}^a$	degree (deg) $[\text{Ga}(\text{dedpa})]^+$
O(1)–Ga–O(2)	101.1	101.39(6)	N(1)–Ga–N(3)	78.9	77.82(6)
O(1)–Ga–N(1)	79.6	80.14(6)	N(2)–Ga–N(3)	111.2	108.92(6)
O(2)–Ga–N(1)	94.1	94.02(6)	O(1)–Ga–N(4)	93.3	90.32(6)
O(1)–Ga–N(2)	91.5	94.73(6)	O(2)–Ga–N(4)	154.7	155.64(6)
O(2)–Ga–N(2)	80.0	79.64(6)	N(1)–Ga–N(4)	109.0	109.11(6)
N(1)–Ga–N(2)	167.7	170.97(6)	N(2)–Ga–N(4)	79.0	78.15(6)
O(1)–Ga–N(3)	155.7	153.44(6)	N(3)–Ga–N(4)	83.1	83.12(6)
O(2)–Ga–N(3)	91.7	94.78(6)			

<sup>a</sup>An average of the three independent units of  $[\text{Ga}(\text{CHXdedpa})][\text{ClO}_4]$  was calculated.

uncoordinated. Indeed, this result is corroborated with the solid-state structure of  $[\text{Ga}(\text{HCHXoctapa})]$  (Figure 6, Table 2), which displays a six-coordinate complex with a  $\text{N}_3\text{O}_3$  donor set provided by an oxygen atom from each acetate carboxylate arm ( $2 \times \text{O}_{\text{Ac-COO}}$ ), both nitrogen atoms from the CHX-en backbone ( $2 \times \text{N}_{\text{en}}$ ), and one picolinate arm providing a nitrogen and oxygen donor ( $1 \times \text{O}_{\text{pyr-COO}}$ ,  $1 \times \text{N}_{\text{pyr}}$ ), while the second picolinic acid arm is situated well away from the coordination sphere. Moreover, the absence of a counterion in the crystallographic unit suggests the Ga complex is neutral, and hence the uncoordinated picolinic acid is protonated in the solid-state structure. At physiological pH ( $\sim 7.4$ ), it would be expected that this uncoordinated picolinic acid arm would be deprotonated and the overall complex charge to be monoanionic.

$\text{H}_4\text{CHXoctapa}$  was also metalated with In(III) to make direct comparisons between  $\text{H}_4\text{octapa}$  and its cyclohexyl derivative. The solution-state  $^1\text{H}$  NMR spectrum of  $[\text{In}(\text{CHXoctapa})]^-$  portrays multiple (static) isomers in solution (Figure 5). On the basis of examination of the  $^1\text{H}$ – $^1\text{H}$  correlations of the COSY NMR (Supporting Information, Figure S28) and  $^1\text{H}$ – $^{13}\text{C}$  correlations of the HSQC NMR (Supporting Information, Figure S30) spectra, the mixture of isomers can be interpreted to be one major symmetric isomer, which may be the eight-coordinate structure, and one (or two) minor asymmetric isomer(s), which may be a seven-coordinate structure in solution, likely with one acetate carboxylate ( $\text{O}_{\text{Ac-COO}}$ ) unbound.

**DFT Structures and Molecular Electrostatic Potential Maps.** A solid-state structure of the likely monoanionic complex  $[\text{In}(\text{CHXoctapa})]^-$  was not obtained; instead, DFT calculations (modeled in water) were performed at the B3LYP level of theory utilizing the 6-31+g(d,p) basis set for the lighter atoms and effective core potential approximation (LanL2DZ) for  $\text{In}^{3+}$ . The DFT structure of  $[\text{In}(\text{CHXoctapa})]^-$  (Figure 7) reveals an eight-coordinate symmetric complex with approximate  $\text{C}_2$  symmetry, showing tight binding of  $\text{In}^{3+}$ . The electrostatic potential map of the complex exhibits a symmetric and relatively even surface charge distribution. A very similar DFT structure was observed for  $[\text{In}(\text{octapa})]^-$ ; <sup>39</sup> in fact, close quantitative comparison of the In–O or In–N bond lengths and relevant  $\text{N}_{\text{en}}$ –In– $\text{N}_{\text{en}}$  angle reveals very little difference between the two calculated structures (Table 3). The biggest differences in bond lengths arise from the In– $\text{N}_{\text{en}}$  bonds, in which the  $[\text{In}(\text{CHXoctapa})]^-$  complex exhibits bonds that are 0.042 Å shorter than the analogous In– $\text{N}_{\text{en}}$  bonds in  $[\text{In}(\text{octapa})]^-$ .

**Thermodynamic Stability.** Stepwise protonation constants ( $\text{pK}_a$ ) (Table 4), formation constants ( $\log K_{\text{ML}}$ ), and  $\text{pM}$  values ( $-\log[\text{M}^{n+}\text{free}]$ ) (Table 5) have been determined for  $\text{H}_2\text{CHXdedpa}$  and  $\text{H}_4\text{CHXoctapa}$  and some metal complexes. Values of  $\text{pM}$  are a more relevant comparative indicator of the extent to which a metal complex is formed in solution as it takes into consideration metal–ligand association, ligand basicity, and metal ion hydrolysis at the biologically relevant pH of 7.4. The higher the  $\text{pM}$  value, the lower the concentration of free unbound metal ions in solution under the specified conditions ( $10 \mu\text{M}$  total ligand,  $1 \mu\text{M}$  total metal ion, pH 7.4,  $25^\circ\text{C}$ ).

The largest variances in  $\text{pK}_a$  values of  $\text{dedpa}^{2-}$  versus  $\text{CHXdedpa}^{2-}$  and  $\text{octapa}^{4-}$  versus  $\text{CHXoctapa}^{4-}$  both arise from the protonation of a  $\text{N}_{\text{en}}$  atom. In both cases, the first  $\text{N}_{\text{en}}$   $\text{pK}_a$  value of the CHX-pa ligand was more basic (9.23 for both  $\text{CHXdedpa}^{2-}$  and  $\text{CHXoctapa}^{4-}$ ) compared to the native achiral ligand (9.00 and 8.59 for  $\text{dedpa}^{2-}$  and  $\text{octapa}^{4-}$ , respectively). These small differences in ligand basicity may arise from the added structural rigidity of the CHX-en backbone compared to the more flexible en backbone.

In vivo, there are many endogenous ligands that can compete for metal-binding from the desired radiometal complex. Specifically, the iron binding protein apo-transferrin also has a high binding affinity for Ga(III) and In(III), because of the physical similarities between Ga(III)/In(III) and Fe(III). Therefore, it is important that the thermodynamic stabilities of the metal–chelate complex be higher than those for any endogenous ligands such as metal-bound transferrin. The thermodynamic stability constant of  $[\text{Ga}(\text{CHXdedpa})]^+$  was determined to be  $\log K_{\text{ML}} = 27.61(8)$  ( $\text{pM} = 26.7$ ), a comparably high value compared to Ga-transferrin or Ga-DOTA (Table 5), yet slightly lower (by less than 1 order of magnitude) than that previously found for  $[\text{Ga}(\text{dedpa})]^+$  ( $\log K_{\text{ML}} = 28.22(8)$ ,  $\text{pM} = 27.4^{38}$ ). One might have expected that the introduction of a “cyclohexyl” backbone would have resulted in a more rigid chelate with preorganized donor atoms leading to a higher thermodynamic stability constant; nonetheless, the thermodynamic stability value of  $[\text{Ga}(\text{CHXdedpa})]^+$  is still exceptionally high compared to the in vivo Ga(III)-competitor transferrin.

The thermodynamic stability constant ( $\log K_{\text{ML}}$ ) of  $\text{CHXoctapa}^{4-}$  with Ga(III) was determined to be 22.32(20) ( $\text{pM} = 21.4$ ), still a comparably high value, but lower than the corresponding  $\text{dedpa}^{2-}$  or  $\text{CHXdedpa}^{2-}$  values, confirming the obvious—the octadentate derivative would be better suited to larger metal ions such as  $\text{In}^{3+}$ ,  $\text{Y}^{3+}$ , and  $\text{Lu}^{3+}$ .

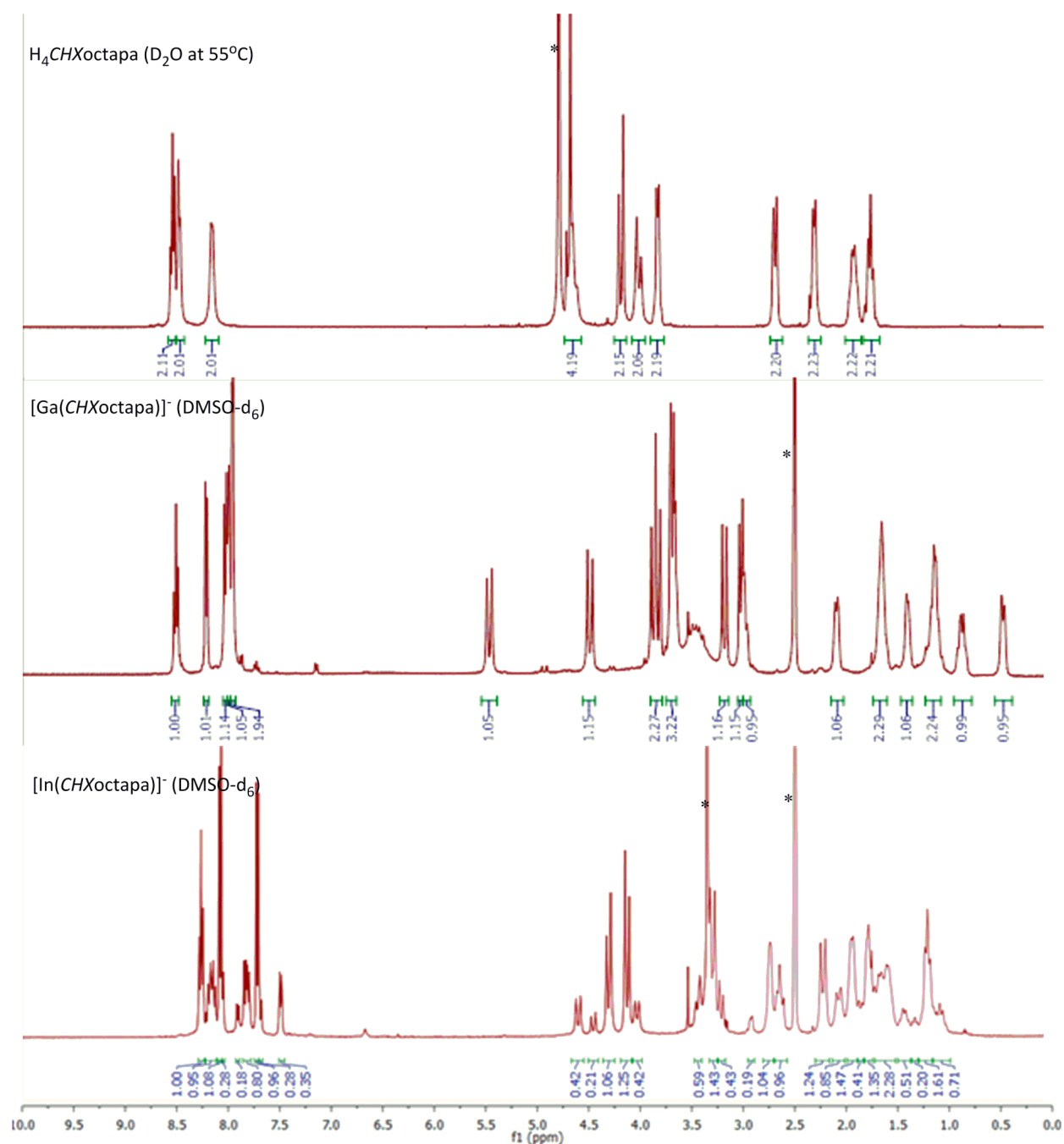


**Figure 5.** <sup>1</sup>H NMR spectra of (top) H<sub>4</sub>CHXoctapa (400 MHz at 55 °C), (middle) [Ga(CHXoctapa)]<sup>-</sup> (400 MHz at 25 °C) showing diastereotopic splitting, and predominantly one isomer in solution, and (bottom) [In(CHXoctapa)]<sup>-</sup> (400 MHz at 25 °C) showing multiple isomers in solution. \*Residual solvent peak.

Much like [In(octapa)]<sup>-</sup> (log  $K_{ML}$  = 26.76(14), pM = 26.5), [In(CHXoctapa)]<sup>-</sup> flaunts exceptionally high thermodynamic stability constants (log  $K_{ML}$  = 27.16(9), pM = 26.3) that exceed those of In-NOTA, In-DOTA, or In-transferrin.

Thermodynamic stability constants are an important factor when evaluating metal-chelate pairs; however, they often do not correlate well with in vivo stability, and serum competition studies are essential experiments to evaluate kinetic inertness of the metal complexes.

**Radiolabeling Experiments.** To determine the ability of the cyclohexyl-pa ligands to label gallium isotopes, the  $\gamma$ -emitter <sup>67</sup>Ga ( $t_{1/2}$  = 3.26 d) was used as a model for <sup>68</sup>Ga in labeling

experiments. The longer half-life of <sup>67</sup>Ga makes it more suitable for in vitro assays than <sup>68</sup>Ga. In addition, because of the success of octapa<sup>4-</sup> with indium(III), the labeling behavior of <sup>111</sup>In with the cyclohexyl derivative CHXoctapa<sup>4-</sup> was also investigated.

Initial radiolabeling experiments discovered H<sub>2</sub>CHXdedpa could quantitatively radiolabel <sup>67</sup>Ga at ambient temperature in 10 min, showing a single sharp peak in the HPLC radiotracer at  $t_R$  = 6.8 min. Concentration-dependent labeling was performed by decreasing the ligand concentration 10-fold, while holding the activity constant (~1 mCi <sup>67</sup>Ga), to determine the highest specific activity (S.A.) and lowest ligand concentration that would yield quantitative labeling. Unlike H<sub>2</sub>dedpa, which exhibited quantitative radiolabeling at ligand concentrations as

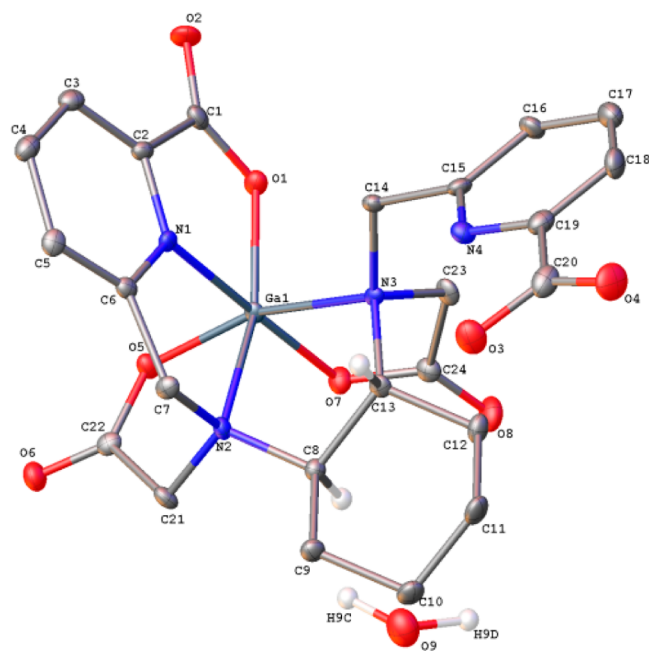


Figure 6. Solid-state structure of  $[\text{Ga}(\text{HCHXoctapa})]\text{H}_2\text{O}$ .

low as  $1 \times 10^{-7}$  M with specific activities as high as 9837 mCi/ $\mu\text{mol}$  at 10 min and room temperature,<sup>38</sup> the analogous cyclohexyl derivative  $\text{H}_2\text{CHXdedpa}$  only radiolabeled quantitatively (>99% radiochemical yield (RCY)) at room temperature with ligand concentrations of  $1 \times 10^{-5}$  M (S.A. 40 mCi/ $\mu\text{mol}$ ); at lower ligand concentrations ( $1 \times 10^{-6}$  M), the RCY was 16% at 10 min and room temperature, and the solution required heating (60 °C, 30 min) to reach an RCY of 96%. Initial radiolabeling studies with the *N*-alkylated derivative  $\text{H}_2\text{CHXdedpa-bb}$  showed <sup>67</sup>Ga labeling of 96% at the original ligand concentration of  $1 \times 10^{-4}$  M, and when ligand concentration was decreased 10-fold to  $1 \times 10^{-5}$  M, radiochemical yield decreased significantly to 27%. The additional benzyl arms of  $\text{H}_2\text{CHXdedpa-bb}$  add a degree of steric hindrance around the metal binding site, which may explain the lower radiochemical yields obtained with the *N*-alkylated derivatives. Additionally, the tertiary backbone nitrogen atoms of  $\text{H}_2\text{CHXdedpa-bb}$  may be inferior electronically to the secondary nitrogen atoms of  $\text{H}_2\text{CHXdedpa}$ , a trend previously observed for  $\text{H}_2\text{dedpa}$  and its derivatives.<sup>38</sup> These results suggest that adding a more rigid chiral backbone onto the chelate structure, making it a more macrocyclic-like ligand, where the cyclohexyl ring acts to preorganize the geometry of the donor atoms, with the intention of adding kinetic inertness, hampers labeling kinetics at low concentrations. The phrase “easy-in, easy-out” may be an applicable catch-phrase for describing radiometal–ligand systems, as a higher energetic barrier to getting a

Table 2. Selected Bond Lengths and Angles in X-ray Structure of  $[\text{Ga}(\text{HCHXoctapa})]$

bond	length (Å)	angle	degree (deg)	angle	degree (deg)
Ga–N(1) <sub>pyr</sub>	1.999(3)	O(7)–Ga–O(5)	92.89(13)	O(5)–Ga–N(2)	82.94(12)
Ga–N(2) <sub>en</sub>	2.152(4)	O(7)–Ga–O(1)	100.01(14)	O(1)–Ga–N(2)	160.52(13)
Ga–N(3) <sub>en</sub>	2.174(3)	O(5)–Ga–O(1)	97.22(12)	N(1)–Ga–N(2)	79.77(14)
Ga–O(1) <sub>pyr-COO</sub>	1.894(3)	O(7)–Ga–N(1)	177.73(14)	O(7)–Ga–N(3)	82.81(13)
Ga–O(5) <sub>Ac-COO</sub>	1.953(3)	O(5)–Ga–N(1)	89.13(13)	O(5)–Ga–N(3)	163.34(12)
Ga–O(7) <sub>Ac-COO</sub>	1.894(3)	O(1)–Ga–N(1)	80.75(14)	O(1)–Ga–N(3)	99.37(13)
		O(7)–Ga–N(2)	99.44(13)	N(1)–Ga–N(3)	94.96(13)
				N(2)–Ga–N(3)	81.92(12)

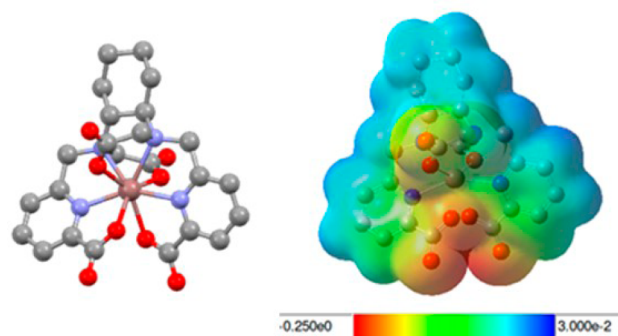


Figure 7. DFT structure of the anion  $[\text{In}(\text{CHXoctapa})]^-$  showing eight-coordinate structure (left), and the molecular electrostatic potential of the complex mapped onto the electron density (right) (positive = blue, negative = red, representing a maximum potential of 0.03 au, and a minimum of  $-0.25$  au, mapped onto electron density isosurfaces of  $0.002 \text{ \AA}^{-3}$ ). Performed using the B3LYP functional employing the 6-31+G(d,p) basis set for first- and second-row elements and LanL2DZ for  $\text{In}^{3+}$  with water as solvent (PCM).

Table 3. Comparison of Relevant Bond Lengths (Å) and Angles (deg) of DFT-Calculated  $\text{In}^{3+}$  Complexes of  $\text{H}_4\text{octapa}^{4-}$  and  $\text{H}_4\text{CHXoctapa}$

bond length (Å)	$[\text{In}(\text{CHXoctapa})]^-$	$[\text{In}(\text{octapa})]^-$
In–O <sub>pyr-COO</sub>	2.309	2.295/2.294
In–O <sub>Ac-COO</sub>	2.224	2.200/2.201
In–N <sub>pyr</sub>	2.244	2.241
In–N <sub>en</sub>	2.496	2.538
N <sub>en</sub> –In–N <sub>en</sub> angle (deg)	76.1	74.8

Table 4. Stepwise Protonation Constants ( $\text{pK}_a$ s) of  $\text{CHXdedpa}^{2-}$  and  $\text{CHXoctapa}^{4-}$

	$\text{CHXdedpa}^{2-}$	$\text{dedpa}^{2-}$ <sup>a</sup>	$\text{CHXoctapa}^{4-}$	$\text{octapa}^{4-}$ <sup>a</sup>
$[\text{H}_6\text{L}]/[\text{H}_5\text{L}][\text{H}]$			1.91(8)	ND
$[\text{H}_5\text{L}]/[\text{H}_4\text{L}][\text{H}]$			1.82(6)	2.79(4)
$[\text{H}_4\text{L}]/[\text{H}_3\text{L}][\text{H}]$	2.40(9)	2.59(6)	2.24(2)	2.77(4)
$[\text{H}_3\text{L}]/[\text{H}_2\text{L}][\text{H}]$	2.99(8)	3.06(6)	3.94(2)	3.77(2)
$[\text{H}_2\text{L}]/[\text{HL}][\text{H}]$	6.47(8)	6.30(5)	5.40(2)	5.59(6)
$[\text{HL}]/[\text{L}][\text{H}]$	9.23(5)	9.00(3)	9.23(1)	8.59(4)

<sup>a</sup>Previously reported values for  $\text{H}_2\text{dedpa}^{38}$  and  $\text{H}_4\text{octapa}^{39}$ . ND = not determined.

radiometal inside a macrocycle (e.g., heating) also often translates to a higher energetic barrier to removing the radiometal from the grasp of the macrocycle (more kinetically inert). An appropriate and functional balance between these forces is much sought after.

**Table 5. Formation Constants ( $\log K_{ML}$ ) and  $pM^a$  Values for  $Ga^{3+}$  and/or  $In^{3+}$  Complexes**

ligand	M = $Ga^{3+}$		M = $In^{3+}$	
	$\log K_{ML}$	$pM^a$	$\log K_{ML}$	$pM^a$
dedpa <sup>2-</sup> 38,39	28.22(8)	27.4	26.60(4)	25.9
CHXdedpa <sup>2-</sup>	27.61(8)	26.7		
octapa <sup>4-</sup> 39			26.76(14)	26.5
CHXoctapa <sup>4-</sup>	22.32(20)	21.4	27.16(9)	26.3
NOTA <sup>51</sup>	30.98	27.9	26.2	23.4
DOTA <sup>52</sup>	21.33	18.5	23.9	18.8
DTPA <sup>53</sup>	24.3	21.0	29.0	25.7
transferrin <sup>54,55b</sup>	20.3	21.3	18.3	18.7

<sup>a</sup>Calculated for 1  $\mu M$  total metal ion, 10  $\mu M$  total ligand, pH 7.4 at 25 °C. <sup>b</sup>Stability constants for highest binding site in *apo*-transferrin.

Initial <sup>67</sup>Ga radiolabeling experiments with H<sub>4</sub>CHXoctapa were similar to those with H<sub>2</sub>CHXdedpa described above. Quantitative radiolabeling (>99% RCY) was achieved at 1 × 10<sup>-4</sup> and 1 × 10<sup>-5</sup> M ligand concentrations with 1–6 mCi <sup>67</sup>Ga, using standard mild labeling conditions (room temperature, 10 min). The RCY decreased to 38% when the ligand concentration decreased to 10<sup>-6</sup> M, with labeling conditions of 10 min at ambient temperature. Labeling yields increased to 72% when the reaction was heated at 70 °C for 1 h. Also, close examination of the labeling peak reveals an interesting split in the radiotracer, likely from different protonation states of the Ga complex in solution; the ligand has an extra carboxylic acid arm that would not be involved in chelation if the predicted six-coordinate complex was formed and therefore could be protonated depending on the pH of the solution. Indeed, the solid-state structure of [Ga(HCHXoctapa)] confirms this hypothesis, since the X-ray structure exhibits a six-coordinate structure with one of the pyridyl carboxylates uncoordinated to the metal center.

Labeling experiments with <sup>111</sup>In and the ligand H<sub>4</sub>CHXoctapa showed quantitative labeling of <sup>111</sup>In at 1 × 10<sup>-4</sup> to 1 × 10<sup>-6</sup> M ligand (>99% RCY) within 10 min at room temperature. The highest specific activity of [<sup>111</sup>In(CHXoctapa)]<sup>-</sup> obtained within 10 min at room temperature was ~670 mCi/ $\mu$ mol (10<sup>-6</sup> M ligand), unlike [<sup>111</sup>In(octapa)]<sup>-</sup>, which yielded specific activities as high as 2300 mCi/ $\mu$ mol at 1 × 10<sup>-7</sup> M ligand concentration, after 10 min at room temperature.

**Human Serum Stability Studies.** To investigate the stability of the <sup>67</sup>Ga and <sup>111</sup>In complexes, a 2 or 120 h competition experiment, respectively, was performed in the presence of excess human blood serum, which contains endogenous ligands that can compete for Ga(III)/In(III) binding *in vivo*/*in vitro*, such as *apo*-transferrin and albumin. This assay is a preferred method of predicting the *in vivo* kinetic inertness of the radiometal ion complexes. Preliminary studies showed that the human serum competition was a harsher competition than the *apo*-transferrin challenge that was used in earlier stability studies with the ligands H<sub>2</sub>dedpa and H<sub>4</sub>octapa. Results for the stability of [<sup>67</sup>Ga(CHXdedpa)]<sup>+</sup>, [<sup>67</sup>Ga(CHXdedpa-bb)]<sup>+</sup>, and [<sup>67</sup>Ga(CHXoctapa)]<sup>-</sup> are compiled in Table 6, with H<sub>2</sub>dedpa, NOTA, and DOTA used as ligand standards for comparison.

The [<sup>67</sup>Ga(CHXdedpa)]<sup>+</sup> complex exhibited excellent stability with 95.7% and 90.5% of <sup>67</sup>Ga remaining chelate bound after 1 and 2 h, respectively; this is a marked improvement compared to the [<sup>67</sup>Ga(dedpa)]<sup>+</sup> complex, which was only 77.8% stable after 2 h. These results clearly show the positive influence on stability that the added chiral modification and preorganization of the

**Table 6. Stability of <sup>67</sup>Ga-Labeled Chelate Ligand Complexes in Human Serum at 37 °C**

complex	1 h (%)	2 h (%)
[ <sup>67</sup> Ga(CHXdedpa)] <sup>+</sup>	95.7 ± 0.7	90.5 ± 4.4
[ <sup>67</sup> Ga(CHXdedpa-bb)] <sup>+</sup>	81.2 ± 3.9	82.9 ± 1.8
[ <sup>67</sup> Ga(CHXoctapa)] <sup>-</sup>	78.1 ± 3.7	74.7 ± 3.5
[ <sup>67</sup> Ga(dedpa)] <sup>+</sup>	94.8 ± 3.4	77.8 ± 1.5
[ <sup>67</sup> Ga(NOTA)]	97.5 ± 0.7	98.0 ± 0.6
[ <sup>67</sup> Ga(DOTA)] <sup>-</sup>	80.1 ± 0.8	80.0 ± 1.9

metal binding site has on complex stability of the dedpa<sup>2-</sup> core. The [<sup>67</sup>Ga(CHXdedpa)]<sup>+</sup> complex also exhibited higher stability (~10% more stable) than the industry gold-standard [<sup>67</sup>Ga(DOTA)]<sup>-</sup> in the human serum stability challenge after 2 h.

A small loss of stability was seen with the benzyl-functionalized derivative H<sub>2</sub>CHXdedpa-bb with only 83% of <sup>67</sup>Ga bound after 2 h. The loss of stability with the *N*-alkylated derivative was also seen in the native H<sub>2</sub>dedpa derivatives previously reported, where stability dropped from >99 to 51% for the H<sub>2</sub>dedpa-bb-NO<sub>2</sub> derivative in a 2 h *apo*-transferrin challenge assay. This may suggest that functionalization at the secondary nitrogen atoms is negatively affecting the coordination sphere of the metal ion and is thus not an appropriate choice for preparing bifunctional derivatives (either due to steric bulk or electronic changes from secondary to tertiary amines, *vide supra*). Moreover, benzyl groups as a model placeholder for bifunctional derivatives may not be an appropriate choice since they introduce a great deal of steric hindrance near the metal binding core, and instead alkyl groups may be a better choice for *N*-alkylation. Nonetheless, alternate modes of functionalization may be required, for example, functionalization on the pyridyl ring, or the cyclohexyl ring to avoid loss of radiometal complex stability.

The <sup>67</sup>Ga-CHXoctapa complex was 74% stable after 2 h. The additional chelating arms of the octadentate chelate, which most likely remain unbound to the metal, may create uneven charge distribution on the metal complex and an easy site for attack of endogenous ligands. Additionally, the decreased stability could simply be a result of modifying the secondary amines of CHXdedpa<sup>2-</sup> to the tertiary amines of CHXoctapa<sup>4-</sup>, which appear to be inferior Ga(III) binding groups. It has been a recurring trend throughout our studies with Ga(III) that ligands that possess secondary amines in their backbone (e.g., H<sub>2</sub>dedpa) have superior stability to those that are functionalized to possess tertiary amines. This trend where the electronics of secondary versus tertiary amine binding groups strongly affects radiometal stability is also observed with <sup>64</sup>Cu binding TETA derivatives, such as CB-TE2A, MM-TE2A, and DM-TE2A, where tertiary amines are found to be far more stable than secondary amines.<sup>32,35</sup> One might expect that H<sub>4</sub>CHXoctapa would be better suited for larger metal ions that can tolerate or prefer higher denticity ligands, ions such as In<sup>3+</sup>. Indeed, the [<sup>111</sup>In(CHXoctapa)]<sup>-</sup> complex showed excellent stability of 91% over 5 d against human serum (Table 7). This result is comparable to those obtained for mouse serum competition assays of <sup>111</sup>In-octapa complexes,<sup>39,41</sup> suggesting H<sub>4</sub>CHXoctapa is a good candidate for further testing *in vivo*.

## CONCLUSIONS

Preliminary investigations of the chiral hexadentate chelating ligand H<sub>2</sub>CHXdedpa (N<sub>4</sub>O<sub>2</sub>) with <sup>67</sup>Ga/Ga<sup>3+</sup> and chiral octadentate chelating ligand H<sub>2</sub>CHXoctapa (N<sub>4</sub>O<sub>4</sub>) with <sup>111</sup>In/In<sup>3+</sup> have shown them to be promising candidates for

Table 7. Stability of  $^{111}\text{In-CHXoctapa}$  in Human Serum at 37 °C and Previously Reported  $^{111}\text{In-octapa}$  Derivatives in Mouse Serum

complex	1 h (%)	24 h (%)	120 h (%)
$^{111}\text{In}(\text{CHXoctapa})^-$	90.9 ± 0.3	90.2 ± 0.5	91.0 ± 0.2
$^{111}\text{In}(\text{octapa})^-$ <sup>39</sup>	93.8 ± 3.6	92.3 ± 0.04	ND <sup>a</sup>
$^{111}\text{In}(\text{octapa-Trastuzumab})^-$ <sup>41</sup>	ND <sup>a</sup>	ND <sup>a</sup>	94.9 ± 0.6
$^{111}\text{In}(\text{DOTA})^-$ <sup>39</sup>	89.6 ± 2.2	89.4 ± 2.2	ND <sup>a</sup>
$^{111}\text{In}(\text{DTPA})^{2-}$ <sup>39</sup>	86.5 ± 2.2	88.3 ± 2.2	ND <sup>a</sup>

<sup>a</sup>Not determined.

radiopharmaceutical elaboration. Both chelates retain their ability to quantitatively label their respective isotopes at room temperature within 10 min, a marked advantage over many of the macrocyclic gold standards such as NOTA and DOTA, and even some new Ga(III) ligands such as TRAP.<sup>29,56</sup>

In vitro human serum stability assays demonstrated  $\text{H}_2\text{CHXdedpa}$  to have improved stability with  $^{67}\text{Ga}$  compared to its achiral counterpart  $\text{H}_2\text{dedpa}$ , with only 9% of  $^{67}\text{Ga}$  transchelated to serum proteins after 2 h versus 22% for  $\text{H}_2\text{dedpa}$ . Moreover, analogous in vitro studies of  $\text{H}_4\text{CHXoctapa}$  with  $^{111}\text{In}$  demonstrated exceptional stability of the complex over 5 d—matching well with results previously obtained for  $\text{H}_4\text{octapa}$ . These stability assays suggest the added structural modification of the cyclohexyl ring onto the ligand backbone results in metal–ligand complexes of higher stability (in the case of  $\text{H}_2\text{CHXdedpa}$ ) or comparable stability (in the case of  $\text{H}_4\text{CHXoctapa}$ ) evaluated against their ethylenediamine analogues  $\text{H}_2\text{dedpa}$  and  $\text{H}_4\text{octapa}$ . Thermodynamic stability constants of  $[\text{Ga}(\text{CHXdedpa})]^+$  and  $[\text{In}(\text{CHXoctapa})]^-$  were determined through potentiometric titrations to be  $\log K_{\text{ML}} = 27.61(8)$  and  $27.16(9)$  ( $\text{pM} = 26.7$  and  $26.3$ ), respectively. The  $[\text{Ga}(\text{CHXdedpa})]^+$  thermodynamic stability constant is comparable to the high stability constant previously obtained for  $[\text{Ga}(\text{dedpa})]^+$  ( $\log K_{\text{ML}} = 28.11(8)$ ,  $\text{pM} = 27.4$ ), further exemplifying the  $\text{CHXdedpa}^{2-}$  scaffold as a strong  $\text{Ga}^{3+}$  ligand. The  $[\text{In}(\text{CHXoctapa})]^-$  thermodynamic stability constant was slightly higher than the already exceptionally high stability constants of  $[\text{In}(\text{octapa})]^-$  ( $\log K_{\text{ML}} = 26.76(14)$ ,  $\text{pM} = 26.5$ ), confirming that  $\text{CHXoctapa}^{4-}$  is a remarkably stable ligand for  $^{111}\text{In}/\text{In}^{3+}$  chelation.

The fast and quantitative labeling of Ga(III) or In(III) isotopes, exceptionally high thermodynamic stability constants, and favorable in vitro stability together with facile and good yield syntheses make  $\text{H}_2\text{CHXdedpa}$  and  $\text{H}_4\text{CHXoctapa}$  ideal candidates for incorporation into radiopharmaceutical design.  $\text{H}_4\text{CHXoctapa}$  is of significant interest for future study with isotopes such as  $^{86/90}\text{Y}$  and  $^{177}\text{Lu}$ . To further demonstrate the stability of these radiotracers in a biological system, biodistribution data will be of significance; hence, moving forward, alternate modes of functionalization of the scaffolds with the intention of making bifunctional derivatives would be of great interest for further testing in vivo to fully evaluate the potential of these promising scaffolds.

## EXPERIMENTAL SECTION

**Materials and Methods.** All solvents and reagents were purchased from commercial suppliers (Sigma-Aldrich, TCI America, Fisher Scientific) and were used as received. Human serum was purchased from Invitrogen. NOTA and DOTA were purchased from Macrocylics. The analytical thin-layer chromatography (TLC) plates were aluminum-backed ultrapure silica gel 60 Å, 250  $\mu\text{m}$  thickness; the flash column silica gel (standard grade, 60 Å, 40–63  $\mu\text{m}$ ) was provided by Silicycle.  $^1\text{H}$  and  $^{13}\text{C}$  NMR spectra were recorded at 25 °C unless otherwise noted on

Bruker AV300, AV400, or AV600 instruments; NMR spectra are expressed on the  $\delta$  scale and referenced to residual solvent peaks. Low-resolution mass spectrometry was performed using a Waters ZG spectrometer with an ESCI electrospray/chemical-ionization source, and high-resolution electrospray-ionization mass spectrometry (HR-ESI-MS) was performed on a Micromass LCT time-of-flight instrument at the Department of Chemistry, University of British Columbia. Microanalyses for C, H, and N were performed on a Carlo Erba Elemental Analyzer EA 1108.  $^{67}\text{Ga}$ - or  $^{111}\text{In}$ -(chelate) human serum stability experiments were analyzed using GE Healthcare Life Sciences PD-10 desalting columns (size exclusion for MW < 5000 Da) and counted with a Capintec CRC 15R well counter. The HPLC system used for analysis and purification of nonradioactive compounds consisted of a Waters 600 controller, Waters 2487 dual wavelength absorbance detector, and a Waters delta 600 pump. Phenomenex Synergi Hydro-RP 80 Å columns (250 mm  $\times$  4.6 mm analytical or 250 mm  $\times$  21.2 mm semipreparative) were used for purification of several of the deprotected ligands. Analysis of radiolabeled complexes was carried out using a Phenomenex Synergi 4  $\mu\text{m}$  Hydro-RP 80A analytical column (250  $\times$  4.60 mm 4  $\mu\text{m}$ ) using a Waters Alliance HT 2795 separation module equipped with a Raytest Gabi Star NaI (TI) detector and a Waters 996 photodiode array (PDA).  $^{67}\text{GaCl}_3$  and  $^{111}\text{InCl}_3$  were cyclotron-produced and provided by Nordion as  $\sim 0.1$  M HCl solutions.

*N,N'*-((1*R*,2*R*)-Cyclohexane-1,2-diylo)bis(2-nitrobenzenesulfonamide) (**1**). To a stirred solution of (1*R*,2*R*)-(–)-1,2-diaminocyclohexane (0.33 g, 2.9 mmol) and  $\text{NaHCO}_3$  (1.44 g, 17.2 mmol, 6 equiv) in THF (6 mL) at 0 °C under  $\text{N}_2$ , a solution of 2-nitrobenzenesulfonyl chloride (1.27 g, 5.7 mmol, 2 equiv) in THF (8 mL) was added dropwise. The murky white mixture was allowed to warm to ambient temperature and stirred overnight. The reaction mixture was filtered to remove sodium bicarbonate and was subsequently concentrated in vacuo. The resultant orange oil was purified by column chromatography (CombiFlash  $R_f$  automated column system; 40 g of HP silica; A: hexanes, B: ethyl acetate, 100% A to 100% B gradient) to yield the product **1** as a fluffy white solid (1.01 g, 73%) ( $R_f = 0.63$ , TLC in ethyl acetate).  $^1\text{H}$  NMR (400 MHz,  $\text{CDCl}_3$ )  $\delta$  8.05 (dd,  $J = 7.5$ , 1.4 Hz, 2H), 7.75 (dd,  $J = 7.4$ , 1.6 Hz, 2H), 7.73–7.61 (m, 4H), 5.59 (d,  $J = 7.0$  Hz, 2H), 3.29–3.15 (m, 2H), 1.79 (d,  $J = 12.7$  Hz, 2H), 1.51 (d,  $J = 7.6$  Hz, 2H), 1.36–1.21 (m, 2H), 1.12 (t,  $J = 9.7$  Hz, 2H).  $^{13}\text{C}$  NMR (101 MHz,  $\text{CDCl}_3$ )  $\delta$  147.6, 134.3, 134.0, 133.5, 130.6, 125.6, 57.7, 33.3, 24.1. MS (ES+)  $m/z = 485.2$   $[\text{M} + \text{H}]^+$ .

*Dimethyl 6,6'*-(((1*R*,2*R*)-Cyclohexane-1,2-diylo)bis(((2-nitrophenyl)sulfonyl)azanediyl))-bis(methylene)dipicolinate (**2**). Potassium carbonate (1.5 g, 11.1 mmol, 6 equiv) was added to a stirred solution of **1** (0.898 g, 1.85 mmol) and methyl-6-bromomethyl picolinate<sup>57</sup> (0.853 g, 3.71 mmol, 2 equiv) in acetonitrile (20 mL). The mixture was stirred at 65 °C for 2 d, excess salts were removed by centrifugation (4000 rpm for 10 min) and filtration, and the filtrate was concentrated in vacuo. The crude product was purified by column chromatography (CombiFlash  $R_f$  automated column system; 80 g of HP silica; A: hexanes, B: ethyl acetate, 100% A to 100% B gradient) to yield the product **2** as a fluffy off-white solid (1.37 g, 94%).  $^1\text{H}$  NMR (400 MHz,  $\text{CDCl}_3$ )  $\delta$  7.67 (d,  $J = 7.7$  Hz, 1H), 7.55 (t,  $J = 7.7$  Hz, 1H), 7.40 (dt,  $J = 16.7$ , 8.4 Hz, 4H), 7.13 (t,  $J = 7.0$  Hz, 1H), 5.01 (d,  $J = 17.5$  Hz, 1H), 4.58 (t,  $J = 18.8$  Hz, 1H), 4.21 (s, 1H), 3.70 (s, 3H), 2.39 (d,  $J = 7.3$  Hz, 1H), 1.61 (s, 1H), 1.31 (m, 2H).  $^{13}\text{C}$  NMR (101 MHz,  $\text{CDCl}_3$ )  $\delta$  164.9, 156.2, 147.2, 146.6, 136.9, 134.1, 132.7, 130.9, 126.1, 123.4, 123.2, 59.6, 53.5, 52.2, 49.6, 32.5, 25.1. MS (ES+)  $m/z = 821.3$   $[\text{M} + \text{K}]^+$ ; 805.4  $[\text{M} + \text{Na}]^+$ .

*N,N'*-[6-(Methoxycarbonyl)pyridin-2-yl]methyl-1,2-(1*R*,2*R*)-cyclohexanediamine (**3**). To a solution of 2 (1.16 g, 1.48 mmol) in THF (10 mL) was added thiophenol (313  $\mu$ L, 3.04 mmol, just over 2 equiv) and potassium carbonate (1.22 g, 8.88 mmol, 6 equiv). The reaction mixture was stirred at ambient temperature for 72 h, during which time a slow color change from faint yellow to deep yellow occurred. The salts were removed by filtration after centrifugation (4000 rpm for 10 min), and the filtrate was concentrated in vacuo. The crude product was purified by column chromatography (CombiFlash  $R_f$  automated column system; 24 g of HP silica; A: dichloromethane, B: methanol with 2% triethylamine, 100% A to 25% B gradient) to yield **3** as a yellow oil (0.606 g, 99%).  $^1\text{H}$  NMR (400 MHz,  $\text{CDCl}_3$ )  $\delta$  7.87 (d,  $J$  = 7.5 Hz, 2H), 7.69 (t,  $J$  = 7.7 Hz, 2H), 7.61 (d,  $J$  = 7.4 Hz, 2H), 4.06 (d,  $J$  = 14.9 Hz, 2H), 3.87 (d,  $J$  = 13.5 Hz, 2H), 3.84 (s, 6H), 2.67 (s, 2H), 2.28–2.19 (m, 2H), 2.05 (d,  $J$  = 13.1 Hz, 2H), 1.60 (d,  $J$  = 8.1 Hz, 2H), 1.17–1.04 (m, 2H), 1.03–0.87 (m, 2H).  $^{13}\text{C}$  NMR (101 MHz,  $\text{CDCl}_3$ )  $\delta$  165.7, 161.4, 147.1, 137.3, 125.7, 123.3, 61.3, 52.7, 52.1, 31.5, 24.8. MS (ES+)  $m/z$  = 451.3  $[\text{M} + \text{K}]^+$ .

$\text{H}_2\text{CHXdedpa}\cdot 2\text{HCl}\cdot 2\text{H}_2\text{O}$  (**4**). Compound **3** (0.314 g, 0.76 mmol) was dissolved in HCl (6 M, 5 mL) and refluxed overnight, during which time a white precipitate formed. The resultant mixture was cooled on ice, and the solid was isolated by vacuum filtration and washed with acetone to yield **4** as a white crystalline solid (0.251 g, 67%).  $^1\text{H}$  NMR (300 MHz,  $\text{D}_2\text{O}$ )  $\delta$  8.15 (dt,  $J$  = 15.3, 7.1 Hz, 4H), 7.76 (d,  $J$  = 6.5 Hz, 2H), 4.98 (d,  $J$  = 17.1 Hz, 2H), 4.85 (d,  $J$  = 15.9 Hz, 2H), 3.72–3.56 (m, 2H), 2.50 (d,  $J$  = 12.5 Hz, 2H), 1.87 (d,  $J$  = 9.0 Hz, 2H), 1.61 (d,  $J$  = 8.7 Hz, 2H), 1.27 (t,  $J$  = 9.9 Hz, 2H).  $^{13}\text{C}$  NMR (75 MHz,  $\text{D}_2\text{O}$ )  $\delta$  167.4, 151.6, 146.6, 140.1, 126.8, 125.7, 58.8, 47.8, 28.1, 22.7. Anal. Calcd (found) for  $\text{C}_{20}\text{H}_{24}\text{N}_4\text{O}_4\cdot 2\text{HCl}\cdot 2\text{H}_2\text{O}$ : C, 48.69 (48.90); H, 6.13 (5.99); N, 11.36 (11.37)%. HR-ESI-MS  $m/z$  for  $\text{C}_{20}\text{H}_{25}\text{N}_4\text{O}_4$  ( $\text{M} + \text{H}^+$ ) calcd. (found): 385.1876 (385.1881) (1.3 PPM).

Dimethyl 6,6'-((1*R*,2*R*)-Cyclohexane-1,2-diyldis((2-*tert*-butoxy)-2-oxoethyl)azanediyldi)bis(methylene)dipicolinate (**5**). To a solution of **3** (0.398 g, 0.96 mmol) in acetonitrile (8 mL), *tert*-butylbromoacetate (285  $\mu$ L, 1.93 mmol, 2 equiv) and sodium carbonate (0.610 g, 5.76 mmol, 6 equiv) were added. The reaction mixture was stirred at 60  $^\circ\text{C}$  overnight. Excess salts were removed by filtration, and the filtrate was concentrated in vacuo. The crude oil was purified by column chromatography (CombiFlash  $R_f$  automated column system; 24 g of HP silica; A: dichloromethane, B: methanol, 100% A to 20% B gradient) to yield **5** as a faint yellow oil (0.423 g, 68%).  $^1\text{H}$  NMR (400 MHz,  $\text{CDCl}_3$ )  $\delta$  8.02 (d,  $J$  = 7.8 Hz, 2H), 7.91 (d,  $J$  = 7.5 Hz, 2H), 7.55 (t,  $J$  = 7.7 Hz, 2H), 3.95 (s, 6H), 3.90 (d,  $J$  = 15.0 Hz, 2H), 3.77 (d,  $J$  = 15.0 Hz, 2H), 3.36 (d,  $J$  = 16.8 Hz, 2H), 3.25 (d,  $J$  = 16.8 Hz, 2H), 2.61 (s, 2H), 2.11 (d,  $J$  = 7.1 Hz, 2H), 1.71 (s, 2H), 1.40 (s, 18H), 1.08 (d,  $J$  = 5.8 Hz, 4H).  $^{13}\text{C}$  NMR (101 MHz,  $\text{CDCl}_3$ )  $\delta$  171.5, 166.1, 161.8, 146.8, 137.0, 127.7, 123.6, 80.5, 61.8, 56.1, 52.9, 52.7, 28.2, 26.3, 26.0. MS (ES+)  $m/z$  = 641.6  $[\text{M} + \text{H}]^+$ .

$\text{H}_4\text{CHXoctapa}\cdot 3.5\text{HCl}\cdot 0.5\text{H}_2\text{O}$  (**6**). Compound **5** (0.336 g, 0.52 mmol) was dissolved in HCl (6 M, 10 mL) and refluxed overnight. The reaction mixture was concentrated in vacuo and purified via semipreparative RP-HPLC (gradient: A: 0.1% TFA (trifluoroacetic acid) in water, B:  $\text{CH}_3\text{CN}$ , 5 to 100% B linear gradient over 25 min, 10 mL/min,  $t_R$  = 12.5 min). Product fractions were pooled, concentrated in vacuo, dissolved in  $\text{CH}_3\text{CN}$  (3 mL) and HCl (3 M, 3 mL), and then concentrated in vacuo again to remove trifluoroacetic acid. This process was repeated two more times; the last time, solvent was lyophilized to yield the HCl salt **6** as an off-white solid (0.136 g, 41% based on MW calculated from EA).  $^1\text{H}$  NMR (400 MHz,  $\text{D}_2\text{O}$ , 55  $^\circ\text{C}$ )  $\delta$  8.54 (t,  $J$  = 7.7 Hz, 2H), 8.48 (d,  $J$  = 7.1 Hz, 2H), 8.16 (d,  $J$  = 5.4 Hz, 2H), 4.74–4.57 (m, 4H), 4.19 (d,  $J$  = 17.4 Hz, 2H), 4.01 (d,  $J$  = 17.1 Hz, 2H), 3.83 (d,  $J$  = 9.2 Hz, 2H), 2.69 (d,  $J$  = 12.3 Hz, 2H), 2.31 (d,  $J$  = 8.5 Hz, 2H), 1.93 (d,  $J$  = 8.9 Hz, 2H), 1.83–1.67 (m, 2H).  $^{13}\text{C}$  NMR (101 MHz,  $\text{D}_2\text{O}$ )  $\delta$  172.4, 165.3, 152.5, 146.2, 143.7, 129.1, 126.2, 100.1, 63.3, 52.3, 24.5, 24.4. Anal. Calcd (found) for  $\text{C}_{24}\text{H}_{28}\text{N}_4\text{O}_8\cdot 3.5\text{HCl}\cdot 0.5\text{H}_2\text{O}$ : C, 45.24 (45.26); H, 5.14 (5.47); N, 8.79 (8.41)%. HR-ESI-MS  $m/z$  for  $\text{C}_{24}\text{H}_{29}\text{N}_4\text{O}_8$  ( $\text{M} + \text{H}^+$ ) calcd. (found): 501.1985 (501.1982) (–0.6 PPM).

(1*R*,2*R*)-*N*<sup>1</sup>,*N*<sup>2</sup>-dibenzylcyclohexane-1,2-diamine (**7**). A solution of (1*R*,2*R*)-(–)-1,2-diaminocyclohexane (1.381 g, 12.1 mmol) and benzaldehyde (2.46 mL, 24.2 mmol, 2 equiv) in ethanol (50 mL) was stirred at 0  $^\circ\text{C}$  for 4 h, then overnight at reflux. Formation of imine was

confirmed by MS (ES+)  $m/z$  = 291.4  $[\text{M} + \text{H}]^+$ , and the reaction mixture was cooled to ambient temperature and concentrated in vacuo. The crude imine was purified by column chromatography (CombiFlash  $R_f$  automated column system; 80 g of HP silica; A: dichloromethane, B: methanol, 100% A to 10% B gradient) to yield the intermediate imine as a faint yellow solid (1.28 g). The imine was then dissolved in ethanol (70 mL) at 0  $^\circ\text{C}$ , and  $\text{NaBH}_4$  (0.422 g, 11.2 mmol, ~2.5 equiv) was added in small portions. The mixture was stirred for 2 h, subsequently quenched with saturated aqueous  $\text{NH}_4\text{Cl}$  (70 mL), and extracted with dichloromethane (3  $\times$  90 mL). The organics were collected, dried over  $\text{MgSO}_4$ , and concentrated in vacuo to yield **7** as a yellow oil (1.336 g, 38% over two steps).  $^1\text{H}$  NMR (400 MHz, MeOD)  $\delta$  7.39–7.25 (m, 10H), 3.96 (d,  $J$  = 13.0 Hz, 2H), 3.76 (dd,  $J$  = 12.9, 7.4 Hz, 2H), 2.53–2.41 (m, 2H), 2.21 (d,  $J$  = 12.0 Hz, 2H), 1.83–1.71 (m, 2H), 1.34–1.19 (m, 4H).  $^{13}\text{C}$  NMR (101 MHz, MeOD)  $\delta$  139.3, 129.7, 129.7, 128.7, 60.9, 50.6, 30.8, 25.7. MS (ES+)  $m/z$  = 295.5  $[\text{M} + \text{H}]^+$ .

Dimethyl 6,6'-((1*R*,2*R*)-Cyclohexane-1,2-diyldis(benzylazanediyldi)bis(methylene)dipicolinate (**8**). To a solution of **7** (0.356 g, 1.21 mmol) and methyl-6-bromomethyl picolinate<sup>57</sup> (0.585 g, 2.54 mmol, just over 2 equiv) in acetonitrile (20 mL), potassium carbonate (0.836 g, 6.05 mmol, 6 equiv) was added, and the resultant suspension was refluxed for 3 d. The mixture was cooled to ambient temperature, excess salts were removed by filtration, and filtrate was concentrated in vacuo. The crude yellow oil was purified by column chromatography (CombiFlash  $R_f$  automated column system; 80 g of HP silica; A: dichloromethane, B: methanol, 100% A to 10% B gradient) to yield **8** as a yellow oil (0.537 g, 75%).  $^1\text{H}$  NMR (400 MHz,  $\text{CDCl}_3$ )  $\delta$  7.97 (d,  $J$  = 7.6 Hz, 2H), 7.93 (d,  $J$  = 7.7 Hz, 2H), 7.65 (t,  $J$  = 7.6 Hz, 2H), 7.27 (d,  $J$  = 7.1 Hz, 4H), 7.15–7.07 (m, 6H), 3.98 (s, 6H), 3.84 (d,  $J$  = 15.2 Hz, 2H), 3.72–3.62 (m, 4H), 3.47 (d,  $J$  = 13.6 Hz, 2H), 2.73 (d,  $J$  = 7.0 Hz, 2H), 2.17 (d,  $J$  = 10.0 Hz, 2H), 1.73 (d,  $J$  = 5.4 Hz, 2H), 1.13–0.99 (m, 4H).  $^{13}\text{C}$  NMR (101 MHz,  $\text{CDCl}_3$ )  $\delta$  165.8, 161.8, 147.0, 139.4, 136.6, 128.9, 127.9, 126.8, 126.2, 123.2, 59.1, 55.1, 53.9, 52.7, 25.7, 24.3. (ES+)  $m/z$  = 593.4  $[\text{M} + \text{H}]^+$ .

$\text{H}_2\text{CHXdedpa}\cdot \text{bb}$  (**9**). Compound **8** (0.308 g, 0.52 mmol) was dissolved in THF/water mixture (3:1, 12 mL), and lithium hydroxide (0.062 g, 2.60 mmol, 5 equiv) was added. The mixture was stirred at ambient temperature for 2 h, and solvent was removed in vacuo to yield the product as the lithium adduct.  $^1\text{H}$  NMR (400 MHz, MeOD)  $\delta$  7.95 (d,  $J$  = 7.5 Hz, 2H), 7.87 (d,  $J$  = 7.4 Hz, 2H), 7.77 (t,  $J$  = 7.5 Hz, 2H), 7.24 (d,  $J$  = 6.6 Hz, 4H), 7.14–7.04 (m, 6H), 3.76 (d,  $J$  = 14.5 Hz, 2H), 3.55 (t,  $J$  = 14.9 Hz, 4H), 3.36 (d,  $J$  = 13.4 Hz, 2H), 2.66 (d,  $J$  = 7.8 Hz, 2H), 2.11 (d,  $J$  = 10.3 Hz, 2H), 1.69 (d,  $J$  = 6.1 Hz, 2H), 1.11–0.94 (m, 4H).  $^{13}\text{C}$  NMR (101 MHz, MeOD)  $\delta$  172.8, 161.4, 155.2, 140.8, 138.9, 130.2, 129.1, 128.0, 126.3, 123.4, 60.5, 56.1, 55.1, 26.9, 25.3. The product was then purified via semipreparative RP-HPLC to remove lithium salts (gradient: A: 0.1% TFA (trifluoroacetic acid) in water, B:  $\text{CH}_3\text{CN}$ ; 5 to 100% B linear gradient over 25 min, 10 mL/min,  $t_R$  = 17.9 min). The HPLC fractions were pooled, concentrated in vacuo, redissolved in  $\text{CH}_3\text{CN}$  (1 mL) and HCl (1 M, 3 mL), and concentrated again to drive off trifluoroacetic acid. This process was repeated two more times, and the last time solvent was removed on a lyophilizer yielding the HCl salt **9** as a faint yellow solid (0.143 g, 49%). Anal. Calcd (found) for  $\text{C}_{34}\text{H}_{36}\text{N}_4\text{O}_4\cdot 3.5\text{HCl}\cdot 0.5\text{H}_2\text{O}$ : C, 58.23 (58.58); H, 5.82 (5.93); N, 7.99 (7.96)%. HR-ESI-MS  $m/z$  for  $\text{C}_{34}\text{H}_{37}\text{N}_4\text{O}_4$  ( $\text{M} + \text{H}^+$ ) calcd. (found): 565.2815 (565.2821) (1.1 PPM).

$[\text{Ga}(\text{CHXdedpa})][\text{ClO}_4]$ .  $\text{H}_2\text{CHXdedpa}\cdot 3\text{HCl}$  (**4**) (18.1 mg, 0.037 mmol) was dissolved in methanol/water (1:3, 2 mL); the pH of this solution was 2.5. To this clear solution  $\text{Ga}(\text{ClO}_4)_3\cdot 6\text{H}_2\text{O}$  (14.6 mg, 0.040 mmol, 1.1 equiv) in water (500  $\mu$ L) was added. The pH of this solution was adjusted to 4.5 using NaOH (aq) (0.1 M), and the mixture was stirred at room temperature for 1.5 h. The resultant murky solution was concentrated in vacuo to a white solid. The crude product was dissolved in water/acetonitrile (4 mL: 0.5 mL) and purified by semipreparative RP-HPLC (gradient: A: water, B:  $\text{CH}_3\text{CN}$ , 5 to 100% B linear gradient over 25 min, 10 mL/min,  $t_R$  = 11.3 min). Fractions were concentrated in vacuo and further dried under vacuum overnight to give the product as a white solid (15.7 mg, 77%).  $^1\text{H}$  NMR (400 MHz, dimethyl sulfoxide (DMSO))  $\delta$  8.59 (t,  $J$  = 7.8 Hz, 2H), 8.27 (d,  $J$  = 7.6 Hz, 2H), 8.06 (d,  $J$  = 7.9 Hz, 2H), 5.92 (dd,  $J$  = 10.1, 5.2 Hz, 2H), 4.59

(d,  $J = 17.4$  Hz, 2H), 4.33 (dd,  $J = 17.3, 5.4$  Hz, 2H), 2.31 (d,  $J = 8.3$  Hz, 2H), 2.09–1.97 (m, 2H), 1.78–1.64 (m, 2H), 1.20–1.03 (m, 4H).  $^{13}\text{C}$  NMR (101 MHz, DMSO)  $\delta$  162.5, 150.6, 145.5, 144.5, 127.4, 122.3, 59.0, 45.1, 28.6, 23.9. HR-ESI-MS  $m/z$  for  $\text{C}_{20}\text{H}_{22}^{69}\text{GaN}_4\text{O}_4$  ( $M^+$ ) calcd. (found): 451.0897 (451.0903) (1.3 PPM).

[Ga(CHXdedpa-bb)] $[\text{ClO}_4]$ .  $\text{H}_2\text{CHXdedpa-bb}$  (9) (13.5 mg, 0.024 mmol) was dissolved in methanol/water (1:1). The pH of this solution was adjusted to 3 using HCl (aq) (0.1 M). To this clear solution, a solution of  $\text{Ga}(\text{ClO}_4)_3 \cdot 6\text{H}_2\text{O}$  (17.1 mg, 0.036 mmol, 1.5 equiv) in water (100  $\mu\text{L}$ ) was added, during which time a white precipitate formed. The pH of the solution was adjusted to 4 using NaOH (aq) (0.1 M) and stirred at ambient temperature for 3 h. The precipitate was isolated by centrifugation (4000 rpm, 10 min), the filtrate was decanted, and the solid was dried under vacuum to yield the product as a white powdery solid (16.0 mg, 91%).  $^1\text{H}$  NMR (400 MHz, DMSO)  $\delta$  8.69 (t,  $J = 7.8$  Hz, 1H), 8.35 (d,  $J = 7.5$  Hz, 1H), 8.27 (d,  $J = 7.9$  Hz, 1H), 7.61 (d,  $J = 7.1$  Hz, 2H), 7.37 (dq,  $J = 14.1, 6.9$  Hz, 3H), 4.80 (q,  $J = 18.1$  Hz, 2H), 4.21 (d,  $J = 13.4$  Hz, 1H), 3.46–3.39 (m, 1H), 2.79 (d,  $J = 64.0$  Hz, 1H), 1.24 (d,  $J = 23.6$  Hz, 1H), 1.12 (s, 1H), 1.02–0.85 (m, 2H).  $^{13}\text{C}$  NMR (101 MHz, DMSO)  $\delta$  162.2, 151.9, 146.6, 143.8, 132.9, 131.7, 129.3, 128.5, 127.3, 123.3, 64.5, 62.0, 49.2, 29.3, 23.5. HR-ESI-MS  $m/z$  for  $\text{C}_{34}\text{H}_{34}^{69}\text{GaN}_4\text{O}_4$  ( $M^+$ ) calcd. (found): 631.1836 (631.1837) (0.2 PPM).

[Na[Ga(CHXoctapa)]].  $\text{H}_4\text{CHXoctapa} \cdot 2\text{HCl} \cdot 3\text{H}_2\text{O}$  (6) (14.6 mg, 0.023 mmol) was dissolved in methanol/water (1:1, 1 mL); the pH of this solution was  $\sim 1$ . To this clear solution,  $\text{Ga}(\text{NO}_3)_3 \cdot 6\text{H}_2\text{O}$  (9.6 mg, 0.026 mmol, 1.1 equiv) in water (300  $\mu\text{L}$ ) was added. The pH of the solution was adjusted to 4 using NaOH (aq) (0.1 M), and the mixture was stirred at room temperature overnight, during which time a white precipitate formed. The precipitate was isolated by centrifugation (4000 rpm, 10 min), the filtrate was decanted, and the solid was dried under vacuum to yield the product as a white solid (8.0 mg, 59%).  $^1\text{H}$  NMR (400 MHz, DMSO)  $\delta$  8.51 (t,  $J = 7.7$  Hz, 1H), 8.21 (d,  $J = 7.5$  Hz, 1H), 8.03 (d,  $J = 8.3$  Hz, 1H), 8.00 (d,  $J = 2.7$  Hz, 1H), 7.98–7.93 (m, 2H), 5.46 (d,  $J = 18.9$  Hz, 1H), 4.49 (d,  $J = 18.9$  Hz, 1H), 3.85 (t,  $J = 17.3$  Hz, 2H), 3.74–3.65 (m, 3H), 3.18 (d,  $J = 16.7$  Hz, 1H), 3.02 (d,  $J = 12.8$  Hz, 1H), 3.00–2.93 (m, 1H), 2.09 (d,  $J = 9.7$  Hz, 1H), 1.74–1.60 (m, 2H), 1.40 (d,  $J = 7.6$  Hz, 1H), 1.23–1.08 (m, 2H), 0.87 (dd,  $J = 21.2, 10.0$  Hz, 1H), 0.47 (d,  $J = 10.5$  Hz, 1H).  $^{13}\text{C}$  NMR (101 MHz, DMSO)  $\delta$  170.4, 170.0, 165.5, 163.1, 153.1, 150.1, 147.5, 145.0, 143.0, 138.6, 128.9, 127.0, 124.4, 122.5, 68.0, 63.0, 62.5, 62.5, 54.4, 52.7, 28.0, 26.4, 23.7, 23.6. HR-ESI-MS  $m/z$  for  $\text{C}_{24}\text{H}_{25}^{69}\text{GaN}_4\text{O}_8\text{Na}$  ( $[\text{Ga}(\text{L})^- + \text{H}^+ + \text{Na}^+]$ ) calcd. (found): 589.0826 (589.0831) (0.8 PPM).

[Na[In(CHXoctapa)]].  $\text{H}_4\text{CHXoctapa} \cdot 2\text{HCl} \cdot 3\text{H}_2\text{O}$  (6) (8.2 mg, 0.013 mmol) was dissolved in methanol/water (1:2, 1 mL); the pH of this solution was  $\sim 1$ . To this clear solution,  $\text{In}(\text{ClO}_4)_3 \cdot 8\text{H}_2\text{O}$  (8.7 mg, 0.016 mmol, 1.2 equiv) in water (200  $\mu\text{L}$ ) was added. The pH of this solution was adjusted to 5 using NaOH (aq) (0.1 M) and stirred at 60  $^\circ\text{C}$  for 2 h. The resultant clear solution was evaporated to dryness to yield  $\text{Na}[\text{In}(\text{CHXoctapa})]$ . HR-TOF-MS (ES-)  $m/z$  for  $\text{C}_{24}\text{H}_{24}^{111}\text{InN}_4\text{O}_8$  calcd. (found): 611.0633 (611.0635) (0.3 PPM). Multiple isomers in solution were observed; NMR spectra can be found in the Supporting Information.

**$^{67}\text{Ga}$  or  $^{111}\text{In}$  Radiolabeling Studies.** The ligands  $\text{H}_2\text{CHXdedpa}$ ,  $\text{H}_2\text{CHXdedpa-bb}$ ,  $\text{H}_4\text{CHXoctapa}$ , and standards  $\text{H}_2\text{dedpa}$ ,  $\text{NOTA}$ , and  $\text{DOTA}$  were made up as stock solutions (1 mg/mL,  $\sim 10^{-3}$  M) in deionized water. A 100  $\mu\text{L}$  aliquot of each ligand stock solution was transferred to screw-cap mass spectrometry vials and diluted with pH 4 NaOAc (10 mM) buffer such that the final volume was 1 mL after the addition of  $^{67}\text{GaCl}_3$  or  $^{111}\text{InCl}_3$  to a final ligand concentration of  $\sim 10^{-4}$  M for each sample. An aliquot of  $^{67}\text{GaCl}_3$  or  $^{111}\text{InCl}_3$  ( $\sim 1$  mCi for labeling studies and  $\sim 3$ –6 mCi for serum competitions) was added to the vials containing the ligand and allowed to radiolabel at ambient temperature for 10 min ( $\text{DOTA}$  was reacted at 70  $^\circ\text{C}$ , 30 min), and then it was analyzed by RP-HPLC to confirm radiolabeling and calculate yields. Areas under the peaks observed in the HPLC radiotracer were integrated to determine radiolabeling yields. Elution conditions used for RP-HPLC analysis were gradient: A: 10 mM NaOAc buffer, pH 4, B:  $\text{CH}_3\text{CN}$ ; 0 to 100% B linear gradient 20 min. [ $^{67}\text{Ga}(\text{CHXdedpa})$ ] $^+$  ( $t_R = 6.8$  min), [ $^{67}\text{Ga}(\text{CHXdedpa-bb})$ ] $^+$  ( $t_R = 13.7$  min), [ $^{67}\text{Ga}$

( $\text{CHXoctapa}$ )] $^-$  ( $t_R = 7.1$  min), [ $^{67}\text{Ga}(\text{NOTA})$ ] ( $t_R = 3.6$  min), [ $^{67}\text{Ga}(\text{DOTA})$ ] $^-$  ( $t_R = 3.0$  min), [ $^{111}\text{In}(\text{CHXoctapa})$ ] ( $t_R = 6.6$  min), free  $^{67}\text{Ga}$  or  $^{111}\text{In}$  ( $t_R = 2.0$ –2.4 min).

**Human Serum Stability Data.** The compounds [ $^{67}\text{Ga}(\text{CHXdedpa})$ ] $^+$ , [ $^{67}\text{Ga}(\text{CHXdedpa-bb})$ ] $^+$ , [ $^{67}\text{Ga}(\text{CHXoctapa})$ ] $^-$ , [ $^{67}\text{Ga}(\text{dedpa})$ ] $^+$ , [ $^{67}\text{Ga}(\text{NOTA})$ ], [ $^{67}\text{Ga}(\text{DOTA})$ ] $^-$ , and [ $^{111}\text{In}(\text{CHXoctapa})$ ] $^-$  were prepared with the radiolabeling protocol as described above. Human serum was removed from the freezer and allowed to thaw at ambient temperature. In triplicate for each  $^{67}\text{Ga}$  or  $^{111}\text{In}$  complex above, solutions were prepared in vials with 750  $\mu\text{L}$  of human serum, 500  $\mu\text{L}$  of  $^{67}\text{Ga}$  or  $^{111}\text{In}$  complex, and 250  $\mu\text{L}$  of phosphate buffered saline (PBS) and incubated at 37  $^\circ\text{C}$  in a water bath. At time points 1 and 2 h, 500  $\mu\text{L}$  of the human serum competition mixture was removed from each vial (for  $^{111}\text{In}$  complex competitions 400  $\mu\text{L}$  aliquots of mixture at 1, 24, and 120 h were removed), diluted to a total volume of 2.5 mL with PBS, and then counted in a Capintec CRC 15R well counter to obtain a value for the total activity to be loaded on the PD-10 column. The 2.5 mL of diluted human serum mixture was loaded onto a PD-10 column that had previously been conditioned via elution with 20 mL of PBS, and the empty vial was counted in a well counter to determine the residual activity left in the vial. The 2.5 mL of loading volume was allowed to elute into a waste container, and then the PD-10 column was eluted with 3.5 mL of PBS and collected into a separate vial. The eluent that contained  $^{67}\text{Ga}$  bound/associated with serum proteins (size exclusion for MW < 5000 Da) was counted in a well counter and then compared to the total amount of activity that was loaded on the PD-10 column to obtain the percentage of  $^{67}\text{Ga}$  or  $^{111}\text{In}$  that was bound to serum proteins and therefore no longer chelate-bound.

**Solution Thermodynamics.** The experimental procedures and details of the apparatus closely followed those of our previous study of  $\text{H}_2\text{dedpa}$  with  $\text{Ga}^{3+}$ .<sup>38</sup> Carbonate-free solutions of the titrant, NaOH, were prepared by dilution of 0.1 mol of NaOH analytical standard solution with freshly boiled MQ water (800 mL) under a stream of nitrogen. The solution was standardized using potassium hydrogen phthalate, and the extent of carbonate accumulation was periodically checked by titration with standard hydrochloric acid solution and determination of the corresponding Gran titration plot. Gallium or indium ion solutions were prepared by dilution of the atomic absorption (AA) standard. The exact amount of acid present in the gallium and indium standards was determined by titration of an equimolar solution of M(III) and  $\text{Na}_2\text{H}_2\text{EDTA}$ . The amount of acid present was determined by Gran's method. Potentiometric titrations were performed using a Metrohm Titrando 809 equipped with a Ross combination pH electrode and a Metrohm Dosino 800. Data were collected in triplicate. The titration apparatus consisted of a 10 mL water-jacketed vessel maintained at  $25.0 \pm 0.1$   $^\circ\text{C}$  (water bath). Prior to and during the titration a stream of nitrogen, passed through 50% KOH, was maintained over the solution to exclude any  $\text{CO}_2$ . The ionic strength was maintained at 0.15 M using NaCl. Prior to each potentiometric titration, the electrode was calibrated using a standard HCl solution. Calibration data were analyzed by standard computer treatment provided within the program GLEE<sup>58</sup> to obtain the calibration parameters  $E_0$  and  $\text{p}K_w$ .

The degree of M(III) complexation at even low pH (<2) was too high to determine the stability constants by direct methods, and the ligand–ligand competition method using the known competitor,  $\text{Na}_2\text{H}_2\text{EDTA}$ , was performed instead. Protonation constants of the proligands and stability constants of Ga(III) or In(III) were calculated within the program Hyperquad<sup>59</sup> using previously reported methods.<sup>38</sup> The protonation constants ( $\text{p}K_a$ ) and  $\log K_{ML}$  values with Ga(III) or In(III) for the proligands and previously reported  $\text{H}_2\text{dedpa}$  and  $\text{H}_4\text{octapa}$  for comparison are listed in Supporting Information, Table S1. Also included are the  $\text{p}M$  ( $-\log[M_{\text{free}}]$ ) values, a more relevant indicator of the extent of which a metal complex is formed in solution.

**X-ray Crystallography.** An orange plate crystal of [ $\text{Ga}(\text{CHXdedpa})_3$ ] $[\text{ClO}_4]_3 \cdot 1.5\text{MeOH} \cdot \text{H}_2\text{O}$  having approximate dimensions of  $0.05 \times 0.14 \times 0.41$  mm was grown by slow evaporation in 1:1  $\text{H}_2\text{O}/\text{MeOH}$  and mounted on a glass fiber. Data for [ $\text{Ga}(\text{CHXdedpa})$ ] $[\text{ClO}_4]$  were collected with graphite-monochromated

Mo  $K\alpha$  radiation (0.710 73 Å) at  $-173.0$  °C. The material crystallizes with three crystallographically independent salt moieties in the asymmetric unit. Two perchlorate anions were disordered and were each modeled in two orientations, with restraints applied making all Cl–O distances relatively equivalent. Additionally, the material crystallizes with both water and methanol in the lattice. The asymmetric unit contains one water molecule and approximately 1.5 MeOH molecules. Measurements were made on a Bruker X8 APEX II diffractometer with graphite monochromated Mo  $K\alpha$  radiation (0.710 73 Å). Data were collected and integrated using the Bruker SAINT<sup>60</sup> software package. Data were corrected for absorption effects using the multiscan technique (SADABS<sup>61</sup>), with minimum and maximum transmission coefficients of 0.832 and 0.934, respectively. The data were corrected for Lorentz and polarization effects. The structure was solved by direct methods using SIR-97 and refined using SHELXL-97<sup>62</sup> via the WinGX<sup>63,64</sup> interface. All non-hydrogen atoms were refined anisotropically. All hydrogen atoms, including hydroxyl H atoms, were placed in calculated positions.

A colorless plate crystal of  $C_{24}H_{24}GaN_4O_8 \cdot H_2O$  ([Ga-(HCHXoctapa)]·H<sub>2</sub>O) having approximate dimensions of  $0.06 \times 0.14 \times 0.31$  mm was grown by slow evaporation in 1:1 H<sub>2</sub>O/DMSO and was mounted on a glass fiber. All measurements were made on a Bruker APEX DUO diffractometer with graphite monochromated Mo  $K\alpha$  radiation. The data were collected at a temperature of  $-183.0 \pm 0.1$  °C to a maximum  $2\theta$  value of  $56.7^\circ$ . Data were collected in a series of  $\phi$  and  $\omega$  scans in  $0.5^\circ$  oscillations using 20.0 s exposures. The crystal-to-detector distance was 60.20 mm. Data were collected and integrated using the Bruker SAINT<sup>60</sup> software package. The linear absorption coefficient,  $\mu$ , for Mo  $K\alpha$  radiation is  $12.45$  cm<sup>-1</sup>. Data were corrected for absorption effects using the multiscan technique (SADABS<sup>61</sup>), with minimum and maximum transmission coefficients of 0.737 and 0.928, respectively. The data were corrected for Lorentz and polarization effects. The structure was solved by direct methods.<sup>65</sup> The material crystallizes with one molecule of water in the asymmetric unit. All non-hydrogen atoms were refined anisotropically. All O–H hydrogen atoms were located in difference maps and refined isotropically. All other hydrogen atoms were placed in calculated positions. The absolute configuration, S, R, R, and R at N2, N3, C8, and C13, respectively, were determined on the basis of the refined Flack x-parameter (0.027(6)).<sup>66</sup>

**Molecular Modeling.** Calculations were performed using *Gaussian 09* (Revision D.01)<sup>67</sup> and visualized using either *GaussView* or *WebMO*. The molecular geometries of the ligand, H<sub>4</sub>CHXoctapa, the complexes with In<sup>3+</sup>, and associated electron densities were obtained from DFT calculations, with the B3LYP functional employing the 6-31+G(d,p) basis set for first- and second-row elements, and the ECP basis set, LANL2DZ, for indium.<sup>68,69</sup> Solvent (water) effects were described through a continuum approach by means of the IEF PCM as implemented in G09. The electrostatic potential was mapped onto the calculated electron density surface.

## ■ ASSOCIATED CONTENT

### ● Supporting Information

DFT structure illustrating intramolecular hydrogen bonding, data and figures from potentiometric and <sup>1</sup>H NMR titrations, HPLC radio traces, <sup>1</sup>H/<sup>13</sup>C/COSY/HSQC NMR spectra of several compounds and metal complexes, crystallographic information files (CIF) for the X-ray crystal structures along with relevant distance and bond angle data. This material is available free of charge via the Internet at <http://pubs.acs.org>.

## ■ AUTHOR INFORMATION

### Corresponding Authors

\*Phone: (604) 222-7527. Fax: (604) 222-1074. E-mail: adam@triumf.ca. (M.J.A.)

\*Phone: (604) 822-4449. Fax: (604) 822-2847. E-mail: orvig@chem.ubc.ca. (C.O.)

### Notes

The authors declare no competing financial interest.

## ■ ACKNOWLEDGMENTS

We acknowledge Nordion (Canada) and the Natural Sciences and Engineering Research Council (NSERC) of Canada for grant support (CR&D, Discovery), NSERC for CGS-M/CGS-D fellowships (C.F.R.), and the University of British Columbia for 4YF fellowships (C.F.R. and E.B.). C.O. acknowledges the Canada Council for the Arts for a Killam Research Fellowship (2011–2013). The authors would also like to thank Dr. E. W. Price for thoughtful editing and Dr. D. W. Wester (Nordion) for mentoring and collaboration throughout the project.

## ■ ABBREVIATIONS

CHX, cyclohexyl/cyclohexane

H<sub>2</sub>dedpa, 1,2-[[6-carboxy-pyridin-2-yl]-methylamino]ethane (N<sub>4</sub>O<sub>2</sub>, CN = 6)

H<sub>2</sub>CHXdedpa, cyclohexyl-H<sub>2</sub>dedpa (N<sub>4</sub>O<sub>2</sub>, CN = 6)

H<sub>2</sub>CHXdedpa-bb, *N,N'*-dibenzylated cyclohexyl-H<sub>2</sub>dedpa (H<sub>2</sub>CHXdedpa-*N,N'*-Bn, N<sub>4</sub>O<sub>2</sub>, CN = 6)

H<sub>4</sub>octapa, *N,N'*-bis(6-carboxy-2-pyridylmethyl)-ethylenediamine-*N,N'*-diacetic acid (N<sub>4</sub>O<sub>4</sub>, CN = 8)

H<sub>4</sub>CHXoctapa, cyclohexyl-H<sub>4</sub>octapa (N<sub>4</sub>O<sub>4</sub>, CN = 8)

EDTA, ethylenediaminetetraacetic acid (N<sub>2</sub>O<sub>4</sub>, CN = 6)

DTPA, diethylenetriaminepentaacetic acid (N<sub>3</sub>O<sub>5</sub>, CN = 8)

CHX-A''-DTPA, cyclohexyldiethylenetriaminepentaacetic acid (N<sub>3</sub>O<sub>5</sub>, CN = 8)

NOTA, 1,4,7-triazacyclononane-1,4,7-triacetic acid (N<sub>3</sub>O<sub>3</sub>, CN = 6)

DOTA, 1,4,7,10-tetraazacyclododecane-1,4,7,10-tetraacetic acid (N<sub>4</sub>O<sub>4</sub>, CN = 8)

TRAP, 1,4,7-triazacyclononane-1,4,7-tris[methyl(2-carboxyethyl)phosphinic acid] (N<sub>3</sub>O<sub>3</sub>, CN = 6)

TETA, 1,4,8,11-tetraazacyclotetradecane-1,4,8,11-tetraacetic acid (N<sub>4</sub>O<sub>4</sub>, CN = 8)

CB-TE2A, 4,11-bis(carboxymethyl)-1,4,8,11-tetraazabicyclo[6.6.2]-hexadecane (N<sub>4</sub>O<sub>2</sub>, CN = 6)

## ■ REFERENCES

- Wadas, T. J.; Wong, E. H.; Weisman, G. R.; Anderson, C. J. *Chem. Rev.* **2010**, *110*, 2858–2902.
- Anderson, C. J.; Welch, M. J. *Chem. Rev.* **1999**, *99*, 2219–2234.
- Rösch, F.; Baum, R. *Dalton Trans.* **2011**, *40*, 6104–6111.
- Bartholomä, M. D.; Louie, A. S.; Valliant, J. F.; Zubieta, J. *Chem. Rev.* **2010**, *110*, 2903–2920.
- Zeglis, B. M.; Lewis, J. S. *Dalton Trans.* **2011**, *40*, 6168–6195.
- Ramogida, C. F.; Orvig, C. *Chem. Commun.* **2013**, *49*, 4720–4739.
- Price, E. W.; Orvig, C. *Chem. Soc. Rev.* **2014**, *43*, 260–290.
- Deri, M. A.; Zeglis, B. M.; Francesconi, L. C.; Lewis, J. S. *Nucl. Med. Biol.* **2013**, *40*, 3–14.
- Shokeen, M.; Wadas, T. J. *Med. Chem.* **2011**, *7*, 413–429.
- Cutler, C. S.; Hennkens, H. M.; Sisay, N.; Huclier-Markai, S.; Jurisson, S. S. *Chem. Rev.* **2013**, *113*, 858–883.
- Bhattacharyya, S.; Dixit, M. *Dalton Trans.* **2011**, *40*, 6112–6128.
- Fani, M.; Andre, J. P.; Maecke, H. R. *Contrast Media Mol. Imaging* **2008**, *3*, 53–63.
- Shetty, D.; Lee, Y.-S.; Jeong, J. M. *Nucl. Med. Mol. Imaging* **2010**, *44*, 233–240.
- Maecke, H. R.; Hofmann, M.; Haberkorn, U. J. *Nucl. Med.* **2005**, *46*, 172–178.
- Eli Lilly. Cardinal Health - List of FDA approved radiopharmaceuticals. Rev. 10 (2014). <http://www.cardinal.com/> (accessed September 2014).
- Ruser, G.; Ritter, W.; Maecke, H. R. *Bioconjugate Chem.* **1990**, *1*, 345–349.
- Andre, P. J.; Maecke, R. H.; Zehnder, M.; Macko, L.; Akyel, G. K. *Chem. Commun.* **1998**, 1301–1302.

- (18) Riesen, A.; Kaden, T. A.; Ritter, W.; Maecke, H. R. *J. Chem. Soc. Chem. Commun.* **1989**, 460–462.
- (19) Brechbiel, M. W.; Gansow, O. A.; Atcher, R. W.; Schlom, J.; Esteban, J.; Simpson, D. E.; Colcher, D. *Inorg. Chem.* **1986**, *25*, 2772–2781.
- (20) Cooper, M. S.; Ma, M. T.; Sunassee, K.; Shaw, K. P.; Williams, J. D.; Paul, R. L.; Donnelly, P. S.; Blower, P. J. *Bioconjugate Chem.* **2012**, *23*, 1029–1039.
- (21) Wu, C.; Kobayashi, S.; Sun, B.; Yoo, T. M.; Paik, C. H.; Gansow, O. A.; Carrasquillo, J. A.; Pastan, I.; Brechbiel, M. W. *Bioorg. Med. Chem.* **1997**, *5*, 1925–1934.
- (22) Camera, L.; Kinuya, S.; Garmestani, K.; Wu, C.; Brechbiel, M. W.; Pai, L. H.; McMurry, T. J.; Gansow, O. A.; Pastan, I.; Paik, C. H.; Carrasquillo, J. A. *J. Nucl. Med.* **1994**, *35*, 882–889.
- (23) Clifford, T.; Boswell, C. A.; Biddlecombe, G. B.; Lewis, J. S.; Brechbiel, M. W. *J. Med. Chem.* **2006**, *49*, 4297–4304.
- (24) Milenic, D. E.; Garmestani, K.; Chappell, L. L.; Dadachova, E.; Yordanov, A.; Ma, D.; Schlom, J.; Brechbiel, M. W. *Nucl. Med. Biol.* **2002**, *29*, 431–442.
- (25) Hens, M.; Vaidyanathan, G.; Zhao, X.-G.; Bigner, D. D.; Zalutsky, M. R. *Nucl. Med. Biol.* **2010**, *37*, 741–750.
- (26) Hassfjell, S.; Brechbiel, M. W. *Chem. Rev.* **2001**, *101*, 2019–2036.
- (27) Burke, B. P.; Clemente, G. S.; Archibald, S. J. *J. Labelled Compd. Radiopharm.* **2014**, *57*, 239–243.
- (28) Bartholomä, M. D. *Inorg. Chim. Acta* **2012**, *389*, 36–51.
- (29) Notni, J.; Simeček, J.; Hermann, P.; Wester, H.-J. *Chem.—Eur. J.* **2011**, *17*, 14718–14722.
- (30) Simeček, J.; Zemek, O.; Hermann, P.; Notni, J.; Wester, H.-J. *Mol. Pharmaceutics* **2014**, *11*, 3893–3903.
- (31) Deri, M. A.; Ponnala, S.; Zeglis, B. M.; Pohl, G.; Dannenberg, J. J.; Lewis, J. S.; Francesconi, L. C. *J. Med. Chem.* **2014**, *57*, 4849–4860.
- (32) Dale, A. V.; Pandya, D. N.; Kim, J. Y.; Lee, H.; Ha, Y. S.; Bhatt, N.; Kim, J.; Seo, J. J.; Lee, W.; Kim, S. H.; Yoon, Y.-R.; An, G. I.; Yoo, J. *ACS Med. Chem. Lett.* **2013**, *4*, 927–931.
- (33) Ma, M. T.; Cooper, M. S.; Paul, R. L.; Shaw, K. P.; Karas, J. A.; Scanlon, D.; White, J. M.; Blower, P. J.; Donnelly, P. S. *Inorg. Chem.* **2011**, *50*, 6701–6710.
- (34) Boros, E.; Rybak-Akimova, E.; Holland, J. P.; Rietz, T.; Rotile, N.; Blasi, F.; Day, H.; Latifi, R.; Caravan, P. *Mol. Pharmaceutics* **2014**, *11*, 617–629.
- (35) Boswell, C. A.; Sun, X.; Nui, W.; Weisman, G. R.; Wong, E. H.; Rheingold, A. L.; Anderson, C. J. *J. Med. Chem.* **2004**, *47*, 1465–1474.
- (36) Ferreira, C. L.; Yapp, D. T.; Lamsa, E.; Gleave, M.; Bensimon, C.; Jurek, P.; Kiefer, G. E. *Nucl. Med. Biol.* **2008**, *35*, 875–882.
- (37) Ferreira, C. L.; Lamsa, E.; Woods, M.; Duan, Y.; Fernando, P.; Bensimon, C.; Kordos, M.; Guenther, K.; Jurek, P.; Kiefer, G. E. *Bioconjugate Chem.* **2010**, *21*, 531–536.
- (38) Boros, E.; Ferreira, C. L.; Cawthray, J. F.; Price, E. W.; Patrick, B. O.; Wester, D. W.; Adam, M. J.; Orvig, C. *J. Am. Chem. Soc.* **2010**, *132*, 15726–15733.
- (39) Price, E. W.; Cawthray, J. F.; Bailey, G. A.; Ferreira, C. L.; Boros, E.; Adam, M. J.; Orvig, C. *J. Am. Chem. Soc.* **2012**, *134*, 8670–8683.
- (40) Bailey, G. A.; Price, E. W.; Zeglis, B. M.; Ferreira, C. L.; Boros, E.; Lacasse, M. J.; Patrick, B. O.; Lewis, J. S.; Adam, M. J.; Orvig, C. *Inorg. Chem.* **2012**, *51*, 12575–12589.
- (41) Price, E. W.; Zeglis, B. M.; Cawthray, J. F.; Ramogida, C. F.; Ramos, N.; Lewis, J. S.; Adam, M. J.; Orvig, C. *J. Am. Chem. Soc.* **2013**, *135*, 12707–12721.
- (42) Boros, E.; Ferreira, C. L.; Yapp, D. T. T.; Gill, R. K.; Price, E. W.; Adam, M. J.; Orvig, C. *Nucl. Med. Biol.* **2012**, *39*, 785–794.
- (43) Price, E. W.; Zeglis, B. M.; Cawthray, J. F.; Lewis, J. S.; Adam, M. J.; Orvig, C. *Inorg. Chem.* **2014**, *53*, 10412–10431.
- (44) Price, E.; Ferreira, C. L.; Adam, M. J.; Orvig, C. *Can. J. Chem.* **2014**, *695*–705.
- (45) Price, E. W.; Zeglis, B. M.; Lewis, J. S.; Adam, M. J.; Orvig, C. *Dalton Trans.* **2014**, *43*, 119–131.
- (46) Boros, E.; Cawthray, J. F.; Ferreira, C. L.; Patrick, B. O.; Adam, M. J.; Orvig, C. *Inorg. Chem.* **2012**, *51*, 6279–6284.
- (47) Boros, E.; Ferreira, C. L.; Patrick, B. O.; Adam, M. J.; Orvig, C. *Nucl. Med. Biol.* **2011**, *38*, 1165–1174.
- (48) Brechbiel, M. W.; Gansow, O. A.; Pippin, C. G.; Rogers, R. D.; Planalp, R. P. *Inorg. Chem.* **1996**, *35*, 6343–6348.
- (49) Ferreiros-Martinez, R.; Esteban-Gomez, D.; Platas-Iglesias, C.; de Blas, A.; Rodriguez-Blas, T. *Dalton Trans.* **2008**, 5754–5765.
- (50) Platas-Iglesias, C.; Mato-Iglesias, M.; Djanashvili, K.; Muller, R. N.; Elst, L. V.; Peters, J. A.; de Blas, A.; Rodriguez-Blas, T. *Chem.—Eur. J.* **2004**, *10*, 3579–3590.
- (51) Clarke, E. T.; Martell, A. E. *Inorg. Chim. Acta* **1991**, *181*, 273–280.
- (52) Clarke, E. T.; Martell, A. E. *Inorg. Chim. Acta* **1991**, *190*, 37–46.
- (53) Gerald, C. F. G. C.; Delgado, R.; Urbano, A. M.; Costa, J.; Jasanada, F.; Nepveu, F. *J. Chem. Soc., Dalton Trans.* **1995**, 327–335.
- (54) Harris, W. R.; Pecoraro, V. L. *Biochemistry* **1983**, *22*, 292–299.
- (55) Harris, W.; Chen, Y.; Wein, K. *Inorg. Chem.* **1994**, *33*, 4991–4998.
- (56) Notni, J.; Hermann, P.; Havlíčková, J.; Kotek, J.; Kubíček, V.; Plutnar, J.; Loktionova, N.; Riss, P. J.; Rösch, F.; Lukeš, I. *Chem.—Eur. J.* **2010**, *16*, 7174–7185.
- (57) Zeng, X.; Coquière, D.; Alenda, A.; Garrier, E.; Prangé, T.; Li, Y.; Reinaud, O.; Jabin, I. *Chem.—Eur. J.* **2006**, *12*, 6393–6402.
- (58) Gans, P.; O'Sullivan, B. *Talanta* **2000**, *51*, 33–37.
- (59) Gans, P.; Sabatini, A.; Vacca, A. *Talanta* **1996**, *43*, 1739–1753.
- (60) SAINT, Version 7.60A; Bruker AXS Inc.: Madison, WI, 1997–2010.
- (61) SADABS, V2008/1; Bruker AXS Inc.: Madison, WI, 2008.
- (62) Sheldrick, G. M. *Acta Crystallogr., Sect. A* **2008**, *64*, 112–122.
- (63) Farrugia, L. J. *J. Appl. Crystallogr.* **1999**, *32*, 837–838.
- (64) Farrugia, L. J. *J. Appl. Crystallogr.* **2012**, *45*, 849–854.
- (65) Altomare, A.; Burla, M. C.; Camalli, M.; Casciarano, G. L.; Giavazzo, C.; Guagliardi, A.; Moliterni, A. G. G.; Polidori, G.; Spagna, R. *J. Appl. Crystallogr.* **1999**, *32*, 115–119.
- (66) Parson, S.; Flack, H. D. *Acta Crystallogr.* **2004**, *A60*, s61.
- (67) Frisch, M. J.; Trucks, G. W.; Schlegel, H. B.; Scuseria, G. E.; Robb, M. A.; Cheeseman, J. R.; Scalmani, G.; Barone, V.; Mennucci, B.; Petersson, G. A.; Nakatsuji, H.; Caricato, M.; Li, X.; Hratchian, H. P.; Izmaylov, A. F.; Bloino, J.; Zheng, G.; Sonnenberg, J. L.; Hada, M.; Ehara, M.; Toyota, K.; Fukuda, R.; Hasegawa, J.; Ishida, M.; Nakajima, T.; Honda, Y.; Kitao, O.; Nakai, H.; Vreven, T.; Montgomery, J. A., Jr.; Peralta, J. E.; Ogliaro, F.; Bearpark, M.; Heyd, J. J.; Brothers, E.; Kudin, K. N.; Staroverov, V. N.; Kobayashi, R.; Normand, J.; Raghavachari, K.; Rendell, A.; Burant, J. C.; Iyengar, S. S.; Tomasi, J.; Cossi, M.; Rega, N.; Millam, J. M.; Klene, M.; Knox, J. E.; Cross, J. B.; Bakken, V.; Adamo, C.; Jaramillo, J.; Gomperts, R.; Stratmann, R. E.; Yazyev, O.; Austin, A. J.; Cammi, R.; Pomelli, C.; Ochterski, J. W.; Martin, R. L.; Morokuma, K.; Zakrzewski, V. G.; Voth, G. A.; Salvador, P.; Dannenberg, J. J.; Dapprich, S.; Daniels, A. D.; Farkas, Ö.; Foresman, J. B.; Ortiz, J. V.; Cioslowski, J.; Fox, D. J. *Gaussian 09*, Revision D.01; Gaussian Inc.: Wallingford, CT, 2009.
- (68) Lee, C.; Yang, W.; Parr, R. *Phys. Rev. B* **1988**, *37*, 785–789.
- (69) Becke, A. D. *J. Chem. Phys.* **1993**, *98*, 5648–5652.